



# Modeling geochemical anomalies of stream sediment data through a weighted drainage catchment basin method for detecting porphyry Cu-Au mineralization



Ehsan Farahbakhsh<sup>a,b,c,\*</sup>, Rohitash Chandra<sup>a,b</sup>, Taymor Eslamkish<sup>c</sup>, R. Dietmar Müller<sup>a</sup>

<sup>a</sup> EarthByte Group, School of Geosciences, University of Sydney, Sydney, Australia

<sup>b</sup> Centre for Translational Data Science, University of Sydney, Sydney, Australia

<sup>c</sup> Department of Mining and Metallurgical Engineering, Amirkabir University of Technology (Tehran Polytechnic), Tehran, Iran

## ARTICLE INFO

### Keywords:

Discrete geochemical mapping  
Stream sediment sampling  
Catchment basin  
Mineralization  
Porphyry Cu–Au

## ABSTRACT

Stream sediment surveying is a geochemical sampling method which is typically applied in the preliminary stages of mineral prospecting. Both continuous and discrete mapping approaches have been proposed to delineate geochemical anomalies at large scales using stream sediment samples. We aim to enhance the efficiency of a recent discrete mapping method called Weighted Drainage Catchment Basin (WDCB) which is independent of sampling sites and density, and has an advantage given that samples may not be uniformly distributed throughout the study area. The Enhanced WDCB (E-WDCB) method can be applied to calculate the weight of each catchment basin using different geochemical parameters such as factor scores. Our study focuses on the factor analysis of three datasets from the Bathurst region, New South Wales, Australia, with different numbers of samples. Different associations of the elements revealed by the factor analysis show that such analyses highly depend on the contributing samples and elements. We propose the Catchment Basin Score (CBS) index to delineate the suitability of sampling in each catchment basin. This index can also be applied to integrate the components resulting from several multivariate analyses on different datasets in a same area. The prediction-area plots show that our proposed method is able to predict a higher percentage of porphyry Cu–Au occurrences in a smaller area compared to other canonical methods, e.g. the median of factor scores in each catchment basin. We demonstrate that prospective areas for porphyry Cu–Au mineralization using the proposed discrete mapping method are also well correlated with volcanic and intrusive rocks.

## 1. Introduction

Geochemical surveys provide efficient spatial data through which corresponding exploration evidence layers could be generated for prospecting mineral deposits (e.g., Agterberg, 1992; Agterberg and Bonham-Carter, 2005; Carranza, 2015, 2011, 2008; Carranza and Laborte, 2015a, 2015b; Liu et al., 2014; Lusty et al., 2012; Wang et al., 2012; Yousefi and Carranza, 2016). Stream sediment surveying is one of the different types of geochemical sampling methods generally applied in preliminary stages of mineral prospecting (Bai et al., 2010; Carranza, 2011; Carranza and Hale, 1997; Cheng, 2007; El-Makky and Sediek, 2012; Wang and Zuo, 2015; Wang et al., 2014; Zheng et al., 2014; Zuo, 2011; Zuo et al., 2009). This type of sampling is used to determine anomalous areas; e.g., catchment basins with anomalous content of indicator elements for vectoring into exposed or concealed ore deposits (Yousefi et al., 2013).

In general, two approaches of continuous and discrete mapping of stream sediment geochemical anomalies have been proposed (Carranza, 2010). Sample Catchment Basins (SCB) (Bonham-Carter, 1994; Bonham-Carter and Goodfellow, 1986, 1984; Carranza, 2010, 2008; Carranza and Hale, 1997; Moon, 1999; Spadoni et al., 2004) and Extended Sample Catchment Basins (Spadoni, 2006) originated from the approaches developed for discrete mapping of stream sediment samples. The SCB method highly depends on the sampling site and density which is a drawback since samples may not be uniformly distributed throughout the study area (Carranza, 2004). Interpolated maps and the SCB method may yield poorly constrained estimates of the geochemical background and thus errors in detecting anomalous areas (Yousefi et al., 2013). Moreover, identifying diluted sources of anomalies is a major problem where the catchment basins of different sizes are sampled and several samples are taken within each one of them (Moon, 1999). Yousefi et al. (2013) proposed a discrete mapping method called

\* Corresponding author at: School of Geosciences, University of Sydney, Sydney, Australia.

E-mail address: [e.farahbakhsh@sydney.edu.au](mailto:e.farahbakhsh@sydney.edu.au) (E. Farahbakhsh).

Weighted Drainage Catchment Basin (WDCB) to map stream sediment samples and geochemical anomalies. The method is independent of the sampling sites to overcome drawbacks of the SCB method and model complex anomaly patterns (Yousefi et al., 2013).

The processes which control the composition of downstream materials are poorly known due to the complicated erosion processes, influence of pollutants and also the composition and distribution of regolith and bedrock (Bogen et al., 1992; Macklin et al., 1994; Spadoni, 2006). Geologic, geomorphologic, topographic, climatic and anthropogenic factors are amongst the most important factors which affect the composition of downstream sediments (Spadoni, 2006). Concentration of the elements in stream sediments, generally decreases by increasing the distance downstream from a source (e.g., ore deposit) (Yousefi et al., 2013). Each stream sediment is influenced by sources present upstream and an ideal sampling point is located on a first order drainage (Marjoribanks, 2010). It should be pointed out that even large anomalies may be rapidly diluted in secondary or tertiary streams. Based on this observation, an index can be defined to determine how much the stream sediment samples can represent the distribution patterns of indicator elements in catchment basins from which they have been collected.

The diversity of data sources often involved in the analysis of stream sediments from a given area makes analyzing and interpreting the data more complicated. In some cases, samples are found to be scattered non-uniformly and the sampling density is highly variable throughout the study area. Therefore, a discrete mapping method such as WDCB is more appropriate since it is independent of the sampling density. There is also another challenge that samples may include concentration values of different set of elements. Accordingly, multivariate analysis of such datasets is not straightforward (Parsa et al., 2016; Yousefi et al., 2013, 2012).

Multivariate analysis of stream sediment samples helps to reveal geochemical signatures of a certain type of mineralization (He et al., 2014; Sadeghi et al., 2013). Factor analysis is a well-known multivariate analysis which has been developed for revealing the element assemblages which are genetically present in target ore deposits (e.g., El-Makky, 2011; He et al., 2013; Kumru and Bakaç, 2003; Parsa et al., 2016; Reimann et al., 2002; Sadeghi et al., 2015; Van Helvoort et al., 2005). There are some challenges with the factor analysis method revealing more than one multi-element association or associations not genetically related to the target ore deposit (Cheng, 2007; Spadoni, 2006; Xie et al., 2010; Yilmaz, 2003; Zuo et al., 2009).

The suitability of stream sediment sampling in each catchment basin is not considered in the WDCB mapping. In this study, we aim to introduce the Enhanced WDCB (E-WDCB) method for discrete mapping of geochemical anomalies using the results from analyzing stream sediment samples collected within the Bathurst 1:250K map sheet, New South Wales, Australia. An index called Catchment Basin Score (CBS) is defined to determine whether a geochemical factor in a catchment basin, such as concentration value of a specific element, can be represented by samples collected. This index is applied to categorize each catchment basin in terms of suitability of stream sediment sampling and to delineate catchment basins which can efficiently contribute to mineral potential mapping. In this study, factor analysis is used as a multivariate technique to extract the most efficient components for prospecting porphyry Cu–Au ore deposits and stream sediment samples are mapped based on the extracted components.

## 2. Geological settings and porphyry Cu–Au mineralization

Our study area is the Bathurst 1:250K map sheet (Fig. 1), located in the east of New South Wales (NSW), Australia, on the western edge of the Great Dividing Range in the Macquarie River plain. The geology of the region is dominated by the Late Proterozoic to Triassic Tasman Fold Belt system (TFB) or Tasmanides. The TFB system includes three fold

belts of Late Proterozoic to Early Paleozoic Kanmantoo Fold Belt, Early to Middle Paleozoic Lachlan Fold Belt, and Early Paleozoic to Triassic New England Fold Belt (Degeling et al., 1986). The Kanmantoo Fold Belt has a very restricted range of mineralization and is characterized by strata-bound copper deposits, whereas the Lachlan and New England Fold Belts have a great variety of metallogenic environments associated with both accretionary and extensional tectonic episodes (Scheibner, 1985). The metallogenesis of the Lachlan Fold Belt is characterized by relatively large base-metal deposits and porphyry copper-gold deposits, whereas the New England Fold Belt is dominated by granitoid metallogenesis (Degeling et al., 1986).

The earliest deposits in the Lachlan Fold Belt are strata-bound Cu and Mn deposits of Cambro-Ordovician age (Gray, 1997). In the Ordovician, Cu deposits were formed in a volcanic arc. In the Silurian, porphyry Cu–Au deposits were formed during the late stages of development of the same volcanic arc. The post-accretionary porphyry Cu–Au deposits were emplaced in the Early Devonian on the sites of the accreted volcanic arc. In the Middle to Late Silurian and Early Devonian, a large number of base metal deposits originated as a result of rifting and felsic volcanism (Degeling et al., 1986).

At least some of the porphyry copper deposits on the Molong Rise in the east of NSW could be Early Devonian in age (McA. Powell, 1976). In the Early Devonian, plutons of intermediate composition with porphyry-style gold and copper mineralization intruded the Ordovician shoshonitic volcanic sequences, on the fragmented Molong Micro-continent. The Copper Hill deposit has been interpreted as Early (or Middle) Devonian age on stratigraphic grounds (Chivas and Nutter, 1975; Gilligan et al., 1976). Host intrusions at Yeoval and Cadia have Early Devonian radiometric ages (Gulson and Bofinger, 1972). The magmas with which the porphyry copper deposits are associated could have been formed by later melting of the rocks of the mature Molong Volcanic Arc (Degeling et al., 1986).

Map of eastern Australia showing permissive tracts for porphyry copper deposits and the study area which is located over the Macquarie tract are presented in Fig. 1. The Ordovician to Early Silurian Macquarie Arc is Australia's most significant porphyry province with total resources greater than 80 Moz of Au and 13 Mt of Cu (Cooke et al., 2007). The Ordovician to Early Silurian Macquarie Arc is an intra-oceanic island arc that is most-widely exposed in the New South Wales section of the Lachlan Fold Belt. Igneous and volcanoclastic rocks of the dismembered Macquarie Arc are exposed in four structural belts of Junee-Narromine Volcanic Belt, Central Molong Volcanic Belt, Rockley-Gulgong Volcanic Belt and Kiandra Volcanic Belt (Glen et al., 2011, 2007).

Geochronological, stratigraphic and geochemical evidence is compatible with an episodic evolution of the Macquarie Arc over a period of approximately 50 million years. The arc-related magmatism ranges in age from Early Ordovician to Early Silurian. The Macquarie Arc is well endowed with large porphyry, skarn and epithermal deposits (Kreuzer et al., 2015). Two well-endowed clusters of Au-rich alkalic porphyries have been delineated in the Cadia and Northparkes districts (Holliday et al., 2002; Lickfold et al., 2007, 2003). Mineralization processes in the Cadia district, located in the study area (Fig. 2), comprise composite, multiphase porphyritic monzonite intrusive complexes that intruded broadly comagmatic shoshonitic volcanic centers between 458 and 437 Ma at depths between 2 and 3 km (Kreuzer et al., 2015). A simplified geological map of the study area is shown in Fig. 2.

## 3. Materials and methods

### 3.1. Sampling and analysis

A large number of stream sediment samples have been collected within the study area and the results of their chemical analyses are available through the Geological Survey of New South Wales (GSNSW)

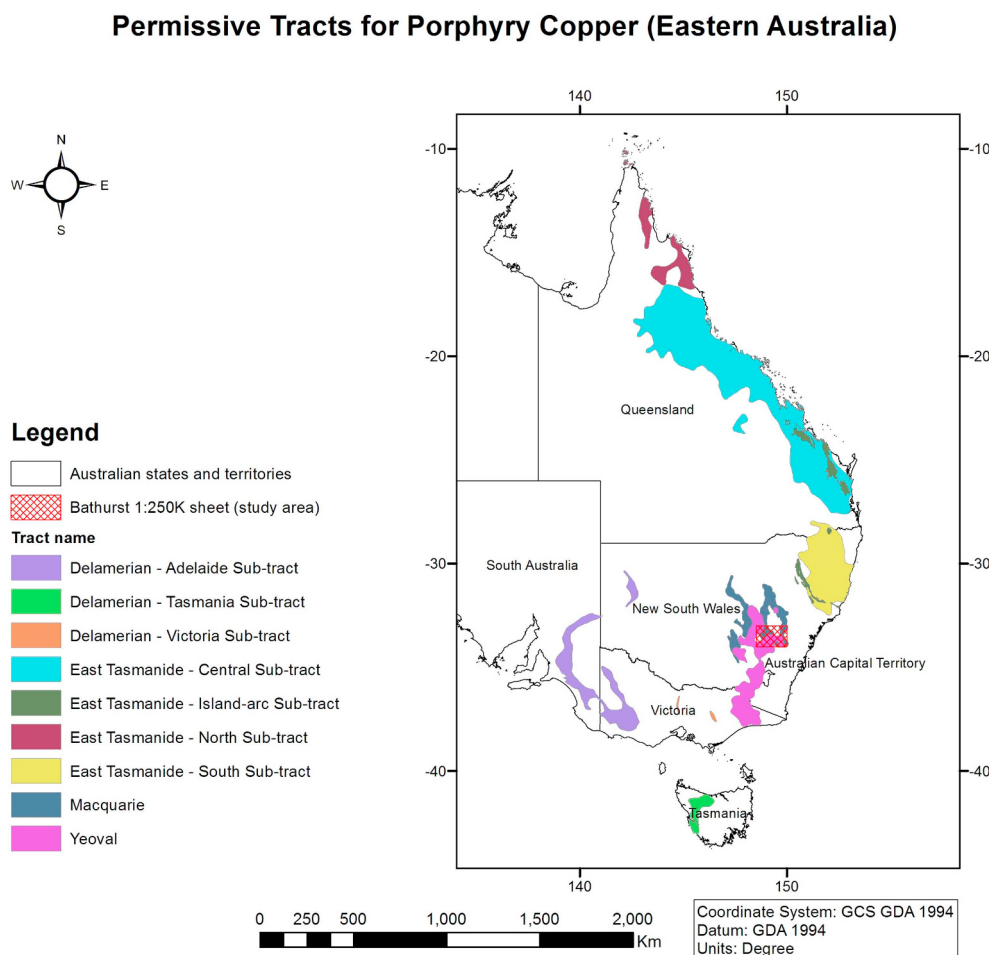


**Fig. 1.** Map of eastern Australia showing permissive tracts for porphyry copper deposits and the Bathurst map sheet study area as red cross-hatched region. (For interpretation of the references to color in this figure legend, the reader is referred to the web version of this article.)  
 (Adapted from Bookstrom et al., 2014.)

Data Warehouse.<sup>1</sup> The samples have been analyzed for determining concentration value of different elements. Here, we selected three subsets containing the results of analyzing associated elements with the porphyry Cu–Au mineralization. The elements of Ag, As, Au, Bi, Co, Cr, Cu, Fe, Mn, Mo, Ni, Pb, S, Sb, W and Zn have been usually selected for uni-, bi- and multivariate processing of the stream sediment samples through prospecting porphyry Cu, Cu–Mo or Cu–Au deposits (e.g., Carranza and Laborte, 2015a; Parsa et al., 2016; Xiao et al., 2014; Yousefi et al., 2013; Zhang and Zhou, 2017). The analyzed elements and number of samples in selected subsets are presented in Table 1. These subsets have been given a name in this table which is used throughout the text for reference. The assay method and detection limit of each element are shown in Table 2.

In this study, streams are delineated based on two data sources. The first is the surface hydrology lines which have been provided by the Geoscience Australia.<sup>2</sup> This dataset presents spatial locations of surface hydrology line features and its attributes at a national scale. It includes natural and man-made geographic features such as watercourses, canals, pipelines, etc. Another source is the ASTER (Advanced Spaceborne Thermal Emission and Reflection Radiometer) Global Digital Elevation Model Version 2 (GDEM) which is freely available from the Earth-Explorer.<sup>3</sup> ASTER's visible and near-infrared subsystem contains nadir-

viewing and backward-viewing telescopes, which together enable its stereoscopic capability to acquire stereo image data with a spatial resolution of nearly 30 m (Farahbakhsh et al., 2016). The streams are extracted initially from the ASTER GDEM and then reconditioned by the surface hydrology lines using Arc Hydro tools. The result is used to outline catchment basins which are used for modeling the geochemical data in this study. Streams with different orders are shown along with the catchment basins in Fig. 3. Also, catchment basins draped over the 2.5-Dimensional (2.5D) topography model of the study area obtained from the ASTER GDEM are shown in this figure.

Every major stream corresponds to a catchment basin. The outlet of each major stream, which is its junction with another major stream, is the starting point to outline the corresponding catchment basin (Yousefi et al., 2013). Geochemical modeling of the stream sediment samples based on the catchment basins in contrast to the sample catchment basin approach does not depend on the location of samples and sampling density. The proposed enhanced WDCB method applied for discrete modeling of the geochemical data is an efficient way to create a geochemical evidential layer to be integrated with other evidential layers through prospecting different types of mineralization such as porphyry Cu–Au. The location of samples draped over the extracted streams and catchment basins can be found separately for each dataset in Fig. 4.

### 3.2. Catchment basin score

The samples in the study area are scattered non-uniformly (Fig. 4).

<sup>1</sup> <http://dwh.minerals.nsw.gov.au>.

<sup>2</sup> <https://data.gov.au/dataset/surface-hydrology-lines-national>.

<sup>3</sup> <http://earthexplorer.usgs.gov>.

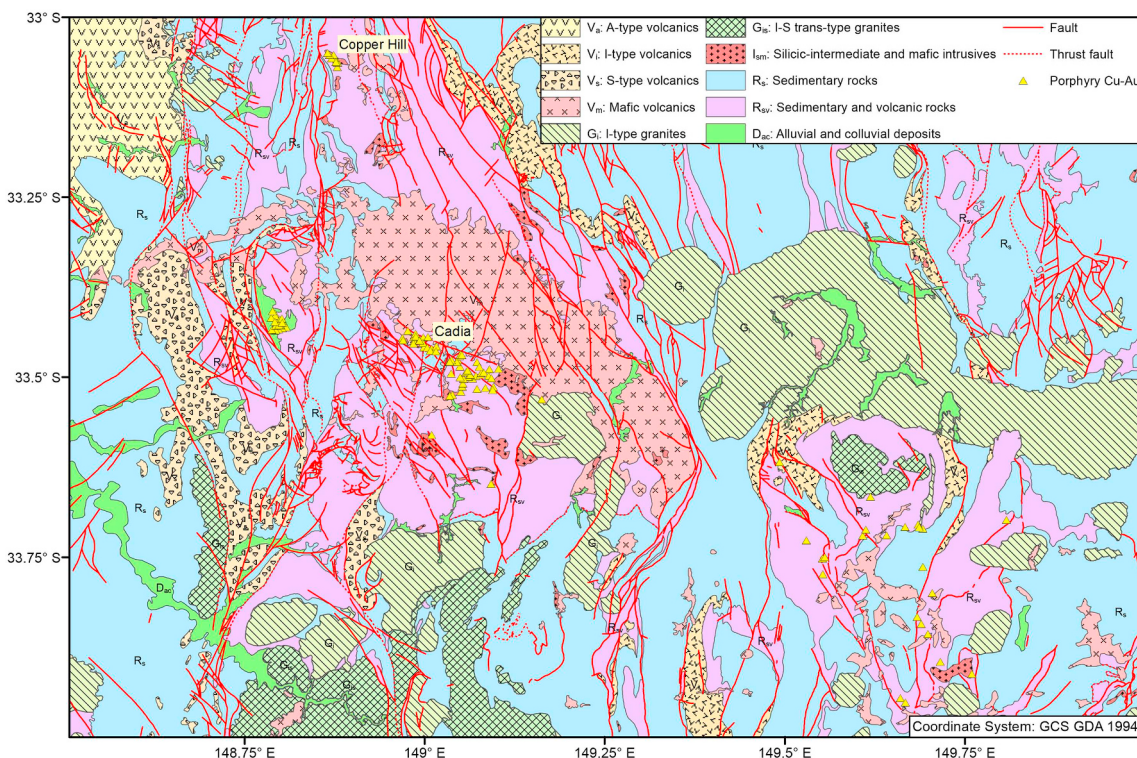


**Fig. 2.** Bathurst 1:250K simplified geological map.  
(Adapted from Raymond and Pogson, 1998.)

**Table 1**  
Properties of the datasets investigated in this study.

Dataset	Elements	Number of samples
A	As, Au, Cu, Pb, Zn	1559
B	As, Co, Cu, Ni, Pb, Zn	2359
C	Cu, Pb, Zn	34,815

**Table 2**  
Assay method and detection limit of each element.

Element	Assay method	Detection limit
As	ICP <sup>a</sup>	0.05 ppm
Au	BLEG <sup>b</sup>	0.01 ppb
Co	AAS <sup>c</sup>	2 ppm
Cu	AAS	2 ppm
Ni	XRF <sup>d</sup>	1 ppm
Pb	AAS	5 ppm
Zn	AAS	5 ppm

<sup>a</sup> Inductively coupled plasma.

<sup>b</sup> Bulk leach extractable gold.

<sup>c</sup> Atomic absorption spectroscopy.

<sup>d</sup> X-ray fluorescence.

It is noticeable that there is different number of samples with different dispersion patterns in each catchment basin. Therefore, it is necessary to define an index by which it can be determined to what extent the samples collected within a catchment basin can represent corresponding geochemical factors such as concentration of a specific element. Concentration of the elements in stream sediments generally decreases by increasing the distance downstream from a source (e.g., ore deposit). Each stream sediment sample is influenced by the sources present at the upstream. The sampling point which is located on a first order drainage is ideal since it is less contaminated by natural or anthropogenic factors (Marjoribanks, 2010). Based on this observation,

most suitable places to take stream sediment samples are within the first-order streams or within the area influenced by these streams. The area influenced by these minor streams can be defined as a buffer zone which surrounds a stream. In this study, the buffer radius is set equal to the one tenth of average distance between centroids of the catchment basins which is 500 m. Also, a buffer zone is defined for each stream sediment sample with similar buffer radius to create two features with the same dimension. The Catchment Basin Score (CBS) can be determined using Eq. (1).

$$CBS_i = \frac{A_{Int}}{A_{Str}} \quad (1)$$

where,  $CBS_i$  is the score of each catchment basin and  $A_{Int}$  is the area of the intersection zone of two buffer zones resulting from the first-order streams and stream sediment samples within each catchment basin.  $A_{Str}$  is the area of the zone influenced by the first-order streams. CBS ranges from 0 to 1. This index shows the suitability of sampling in a specific catchment basin and in addition, it can be used to weigh catchment basins while integrating several discrete geochemical maps. High CBS shows that there are large common areas covered by the first-order streams and the buffer zones of stream sediment samples. Therefore, the collected samples can efficiently represent the catchment basin from which they have been collected. This also implies that the collected samples are weakly influenced by the natural and anthropogenic contamination. The low area of the intersection zones in a catchment basin contributes to low CBS and shows low quality of the stream sediment sampling in terms of sampling location and number which leads to bias results.

### 3.3. Multivariate analysis

Factor analysis as a well-known multivariate analysis method used to reduce variations in multivariate datasets to a few factors to discover hidden multivariate data structures (Johnson and Wichern, 2007; Krumbein and Graybill, 1965; Tripathi, 1979). In this study, it is

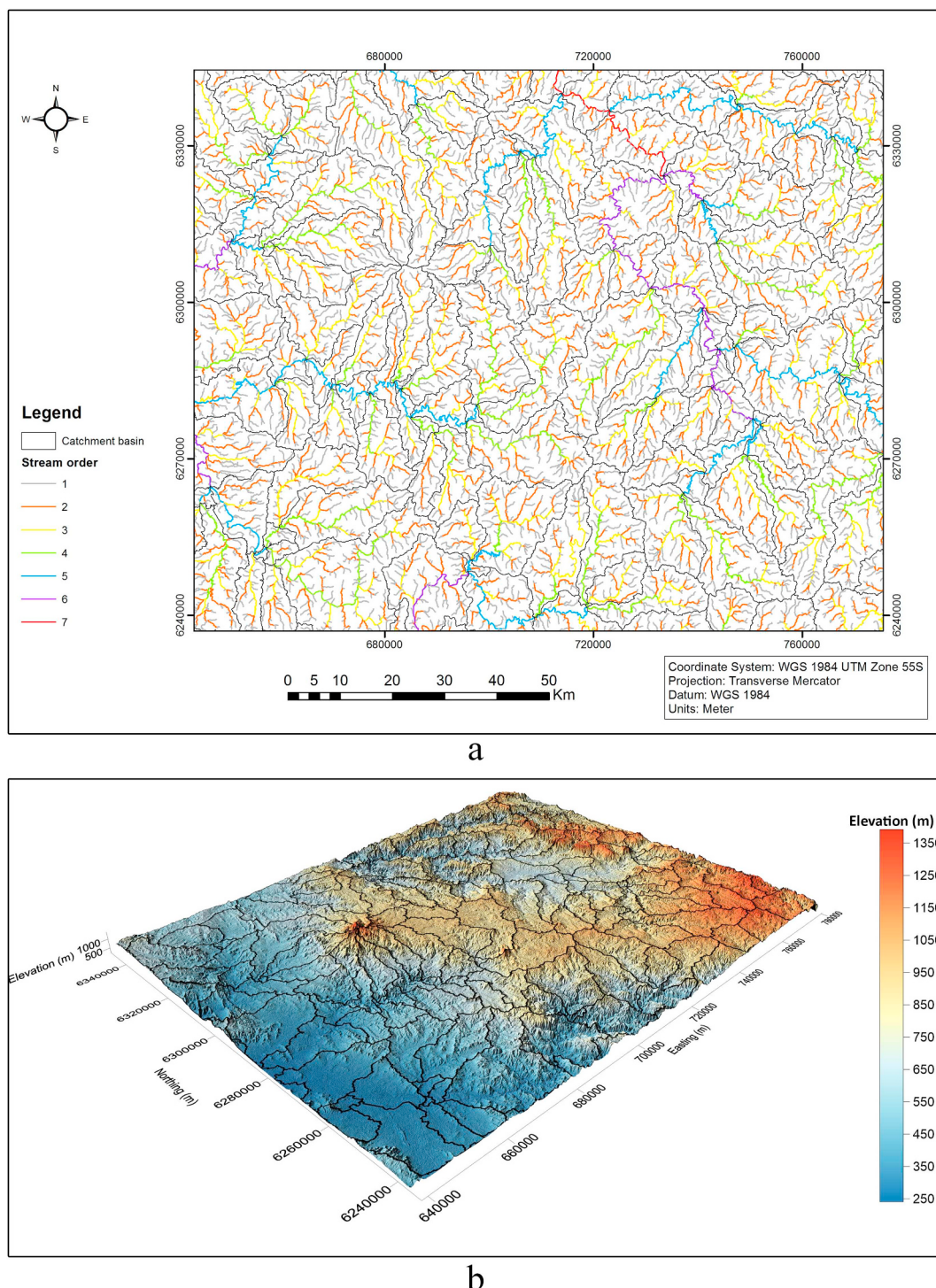


**Fig. 3.** a) Streams with different orders are shown along with the catchment basins; b) catchment basins draped over the 2.5D topography model of the study area obtained from the ASTER GDEM.

applied on the datasets using IBM SPSS Statistics software.<sup>4</sup> Principal Component Analysis (PCA) is used for extracting factors, Varimax is applied as the rotation method (Kaiser, 1958) and a regression method is used to export factor scores. Like many other statistical techniques, factor analysis input data are required to follow a normal or symmetric distribution (Reimann and Filzmoser, 2000). Stream sediment

geochemical data are categorized as compositional data and they represent a closed number system. In this system, individual variables are not independent and they are parts of a whole (Carranza, 2011; Filzmoser et al., 2009a).

Log-ratio transformations are suggested to be applied on the data prior to the factor analysis through opening the close range of variation (Aitchison, 1986; Buccianti, 2015; Buccianti and Grunsky, 2014; Egozcue et al., 2003; Filzmoser et al., 2009c, 2009b, 2009a; Parsa et al., 2016). Different transformation methods have been discussed before to

<sup>4</sup> <https://www.ibm.com/products/spss-statistics>.

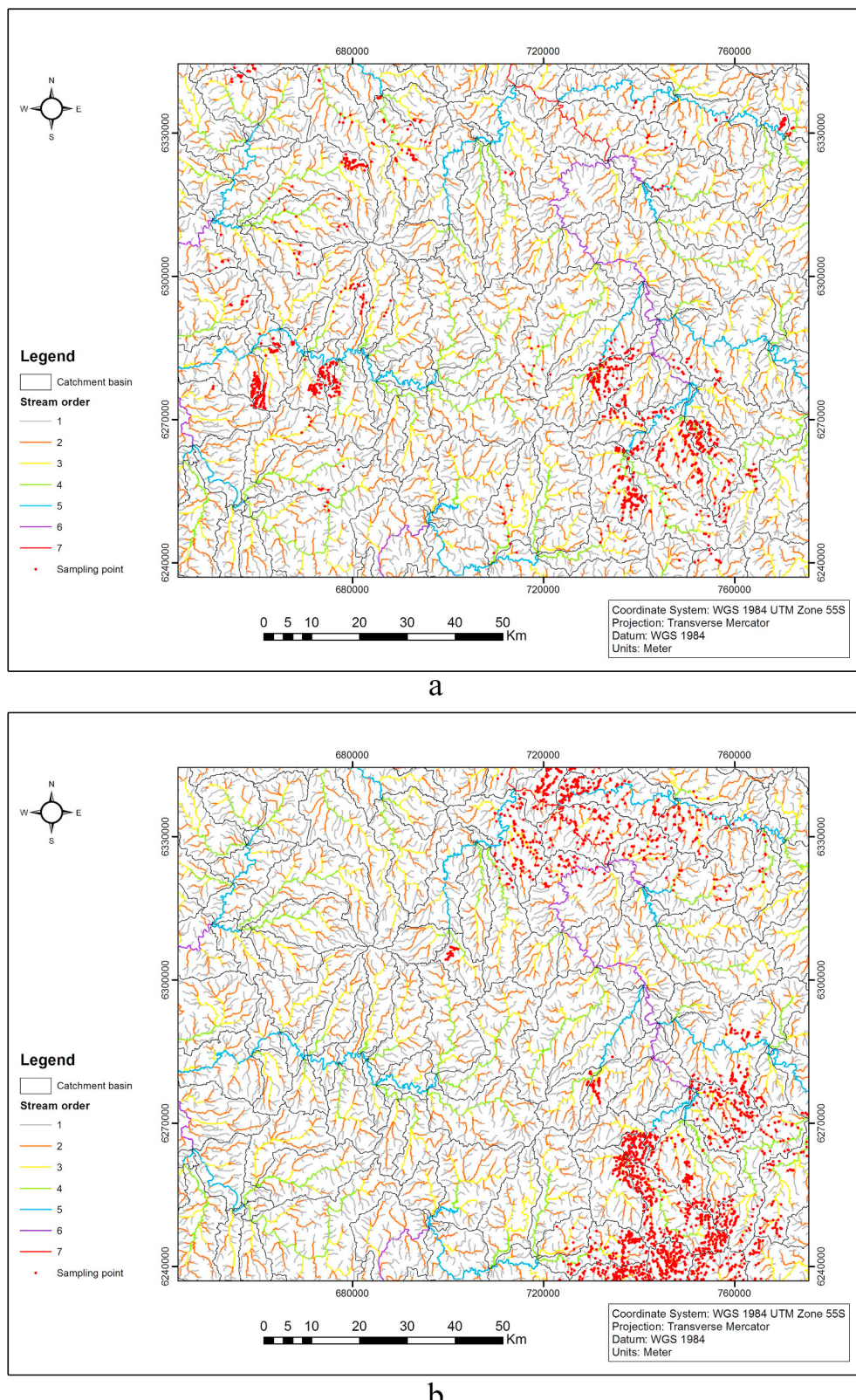
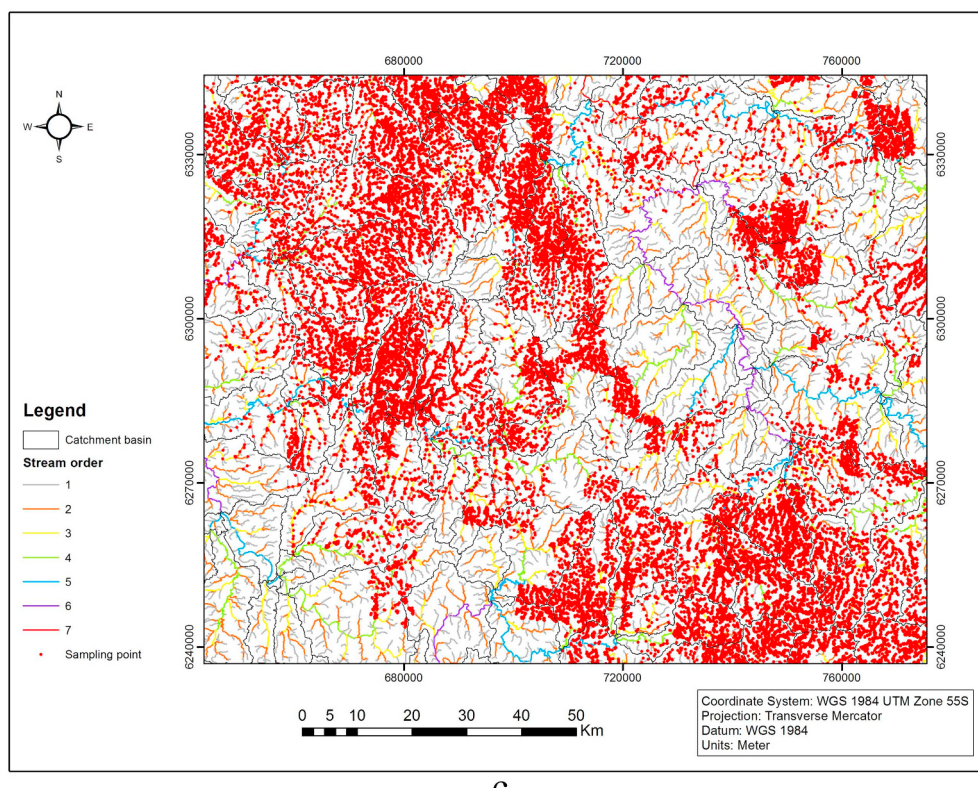


**Fig. 4.** Location of samples from dataset a) A, b) B, and c) C draped over the extracted streams and catchment basins.

reach symmetric distributions from primary geochemical data (e.g., Aitchison and Egoozue, 2005; Templ et al., 2008). Filzmoser et al. (2009a) suggested that the isometric log-ratio (ilr) transformation involves some theoretical advantages over other log-ratio transformations for statistical analysis of the geochemical data.

### 3.4. Discrete geochemical mapping

In general, two approaches have been proposed for mapping stream sediment samples in the literature which consist of continuous and discrete geochemical mapping approaches. According to Carranza



C

Fig. 4. (continued)

**Table 3**

Sample input table to E-WDCB MATLAB program.

Catchment basin ID	Sample ID	Factor score
1	6	-0.166
1	9	-0.405
1	7	1.148
2	1	0.395
2	3	3.239
2	8	-0.103
2	5	1.236
4	2	0.439
4	4	0.155
4	10	2.367
.	.	.
.	.	.
.	.	.

(2010), discrete maps show stronger positive spatial associations with the known mineral occurrences compared to the continuous maps. Yousefi et al. (2013) proposed WDCB method to overcome some drawbacks of the SCB method and delineated complex anomaly patterns independent of the sampling sites.

The topographic and geomorphologic models of a stream network for investigating related features such as geochemical dispersion pattern are based on the catchment basins (Matějíček et al., 2003; Sidorchuk et al., 2003). The stream sediments contain some information about the geochemical characteristics of the catchment basin from which they have been collected, since they are composed of the elements derived not only from the materials within the catchment basin, but erosion and weathering processes also need to be considered (Caranza, 2010; Howarth and Thornton, 1983; Ohta et al., 2005; Xie et al., 2010). According to Spadoni (2006), the spatial influence of a stream sediment sample extends downstream and upstream of a sample location. Hence, stream sediment samples are morphologically influenced by the geochemical characteristics of the relevant catchment

basin.

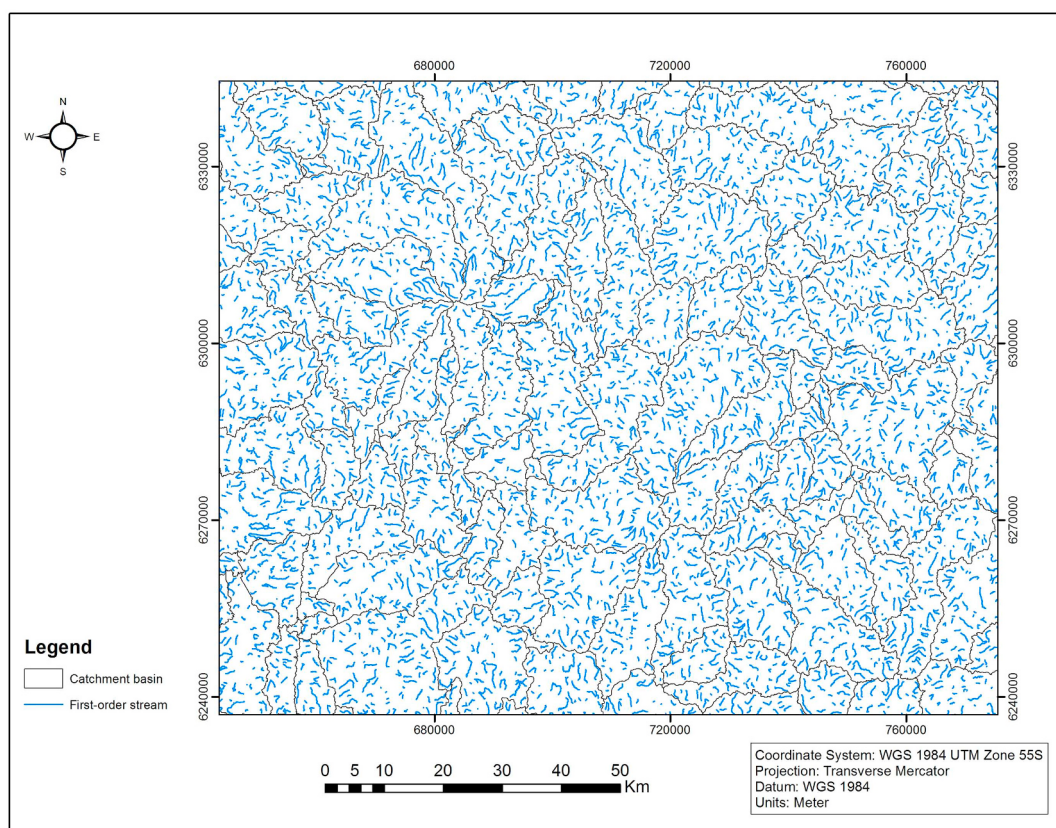
In a WDCB map, a weight is given to the whole of each catchment basin based on this notion that the stream sediments associated with the mineralized catchment basins show higher concentration values of the relevant elements to the target deposit type compared to the ones associated with the non-mineralized catchment basins (Yousefi et al., 2013). Hence, the mean and median of the concentration values of all samples in mineralized catchment basins is higher than the non-mineralized catchment basins. The study area includes 144 catchment basins which are weighted using the E-WDCB method and available data. In this study, factor scores which have been determined using the factor analysis are used instead of the relevant concentration values. The E-WDCB method has been programmed using MATLAB which is available online.<sup>5</sup> The input sample table to this program is shown in Table 3.

The “Factor Score” column in Table 3 can be replaced by any other geochemical parameter for each sampling point. The dataset should be classified first and following percentiles in each dataset are used as the threshold of different classes: 50, 84, 90, 95, 97.5 and 99. In E-WDCB method, the thresholds can be defined arbitrarily in the program which is an improvement compared to Yousefi et al. (2013). Accordingly, there are seven classes for each dataset. If the most anomalous to the most background class be numbered from 1 to n, the weight which is assigned to each catchment basin is determined using Eq. (2) (modified after Yousefi et al., 2013).

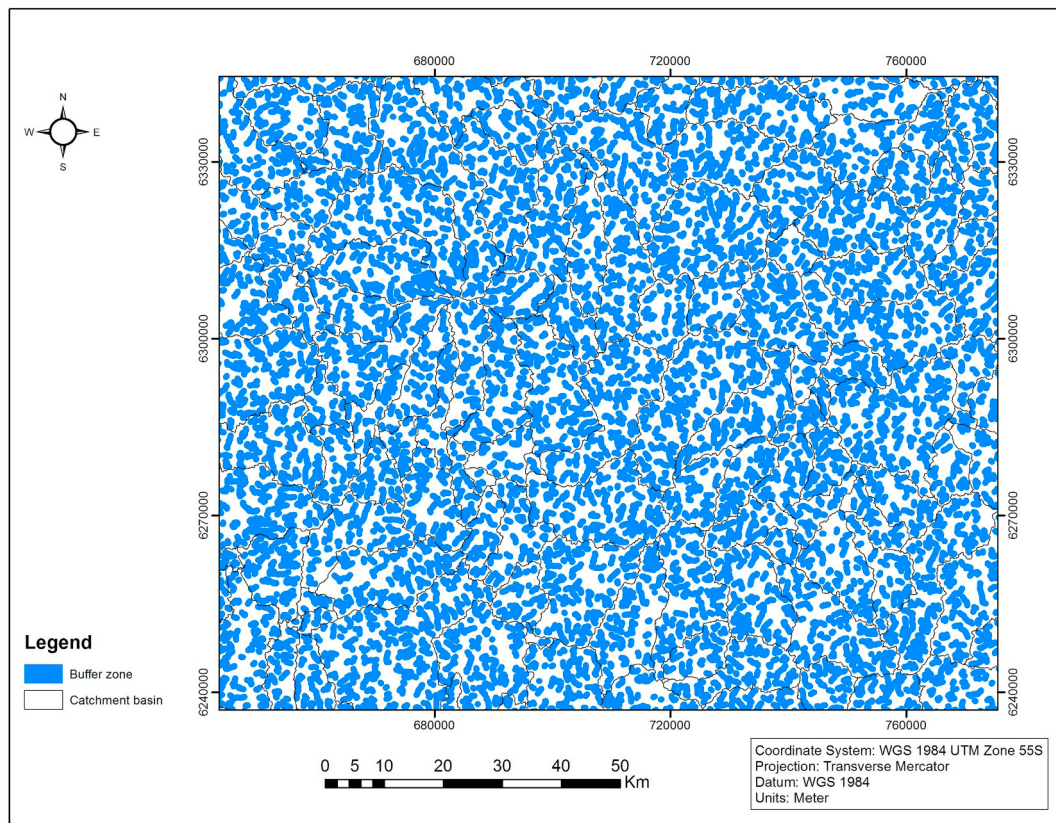
$$w = \sum_{i=1}^n (n - i + 1) \left( M_i \frac{N_i}{N_t} \right) \times 100 \quad (2)$$

here, w is the weight assigned to each catchment basin; i is the index that refers to n number of classes;  $M_i$  is the median or mean of each class;  $N_i$  is the number of samples in each class, and  $N_t$  is the total number of samples within each catchment basin. To assign probabilistic

<sup>5</sup> <https://github.com/intelligent-exploration/3S>.

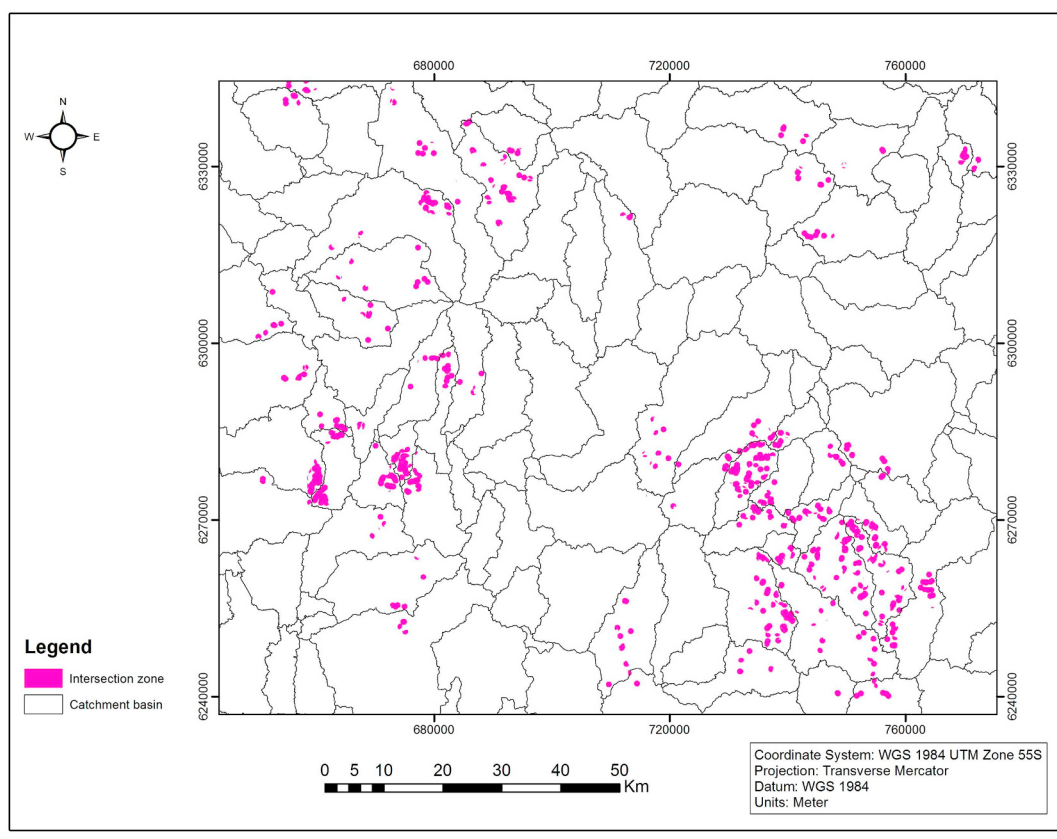


a

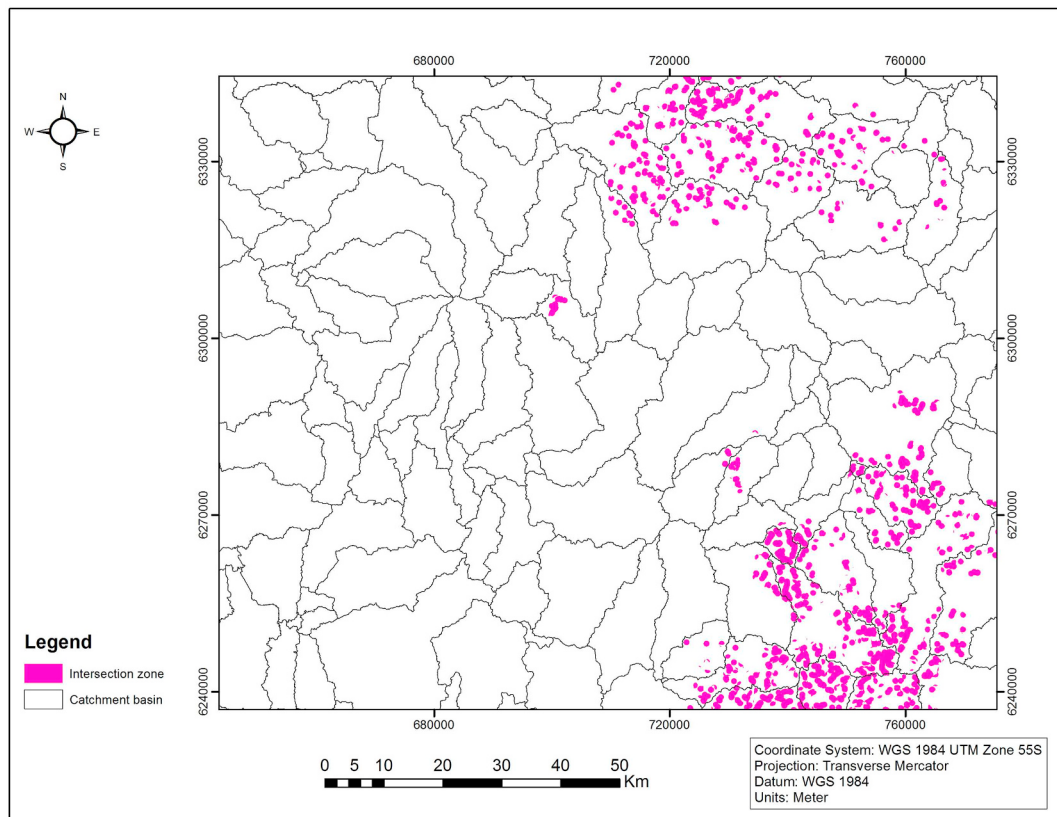


b

**Fig. 5.** a) First-order streams which are considered as the most suitable streams for collecting stream sediment samples; b) buffer zones in a radius of 500 m around the first-order streams.



a



b

**Fig. 6.** Intersection zone of the two buffer zones resulting from the first-order streams and the stream sediment samples within each catchment basin for dataset a), b) B and c) C.

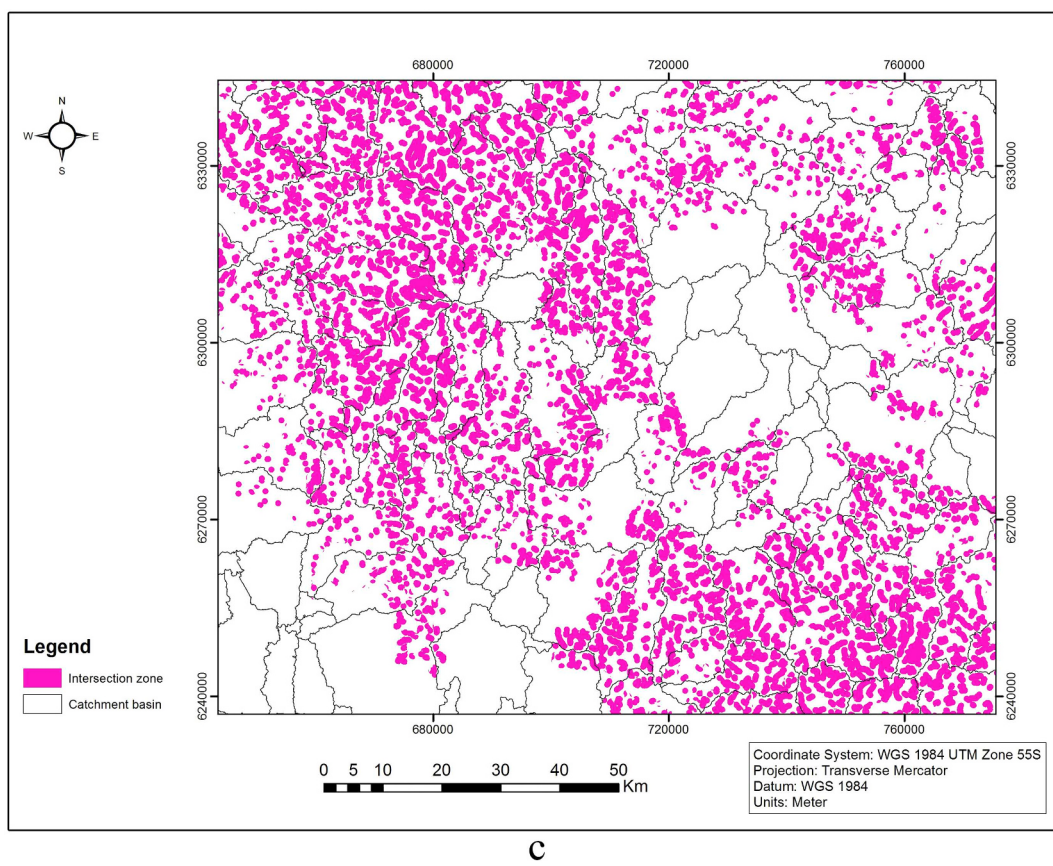


Fig. 6. (continued)

values to each catchment basin in terms of prospecting Au or Cu mineralization, the calculated weights from Eq. (2) are transformed to fuzzy space, which ranges from 0 to 1 using Eq. (3) and called a logistic function (Yousefi and Nykänen, 2016). This transformation not only results in better discrimination of the anomalies from the background level, but also improves the prediction rate of the known mineral occurrences (Parsa et al., 2016; Yousefi et al., 2014; Yousefi and Carranza, 2015a).

$$f_w = \frac{1}{1 + e^{-s(w-i)}} \quad (3)$$

here,  $f_w$  and  $w$  are the transformed and original values, respectively.  $s$  and  $i$  are the slope and inflection point of the logistic function, respectively; which determine the shape of the function and are calculated using Eqs. (4) and (5) (Yousefi and Nykänen, 2016).

$$i = \frac{2 \times \ln 99}{(w) - \min(w)} \quad (4)$$

$$s = \frac{(w) + \min(w)}{2} \quad (5)$$

Eq. (6) is used to determine the overall weight of each catchment basin while integrating several discrete geochemical maps.

$$W = \sum_{i=1}^n \left( \frac{CBS_i}{\sum_{i=1}^n CBS_i} \right) \times w_i \quad (6)$$

here,  $W$  is the overall weight of each catchment basin;  $i$  is the index and ranges from 1 to  $n$ , which is the number of available weights for each catchment basin and it varies from 0 to 3 in this study;  $CBS_i$  is the catchment basin score of each catchment basin in each dataset or map and  $w_i$  is the calculated weight for each catchment basin using Eq. (3).

## 4. Results

### 4.1. CBS index

The Catchment Basin Score (CBS) aims to show the suitability of sampling in a specific catchment basin and in addition, it can be used to weigh catchment basins through integrating multiple discrete geochemical maps. First-order streams are considered as suitable streams for collecting stream sediment samples. In Fig. 5a, they are shown in each catchment basin. Moreover, buffer zones in a radius of 500 m around each first-order stream are mapped in Fig. 5b.

In Fig. 6, intersection zones of two buffer zones resulting from the first-order streams and stream sediment samples within each catchment basin for all three datasets are shown.

The CBS map of each dataset along with the stream sediment samples and corresponding histogram of CBS values are presented in Fig. 7.

In Fig. 7, the CBS values are shown in percent and they can later be used to determine how much the weight assigned to each catchment basin using a discrete mapping method, contributes to mineral potential mapping.

### 4.2. Factor analysis

In this study, ilr-transformed data are used as the input to carry out the factor analysis on all three datasets. Histograms and Quantile-Quantile (Q-Q) plots of the ilr-transformed Au and Cu concentration values from dataset A and ilr-transformed Cu concentration values from datasets B and C are respectively presented in Figs. 8 and 9. According to the histograms, distribution of different datasets show a low skewness near zero and a kurtosis near 3 which are the characteristics of a normal distributed population (Montgomery et al., 2010). Q-Q plots are

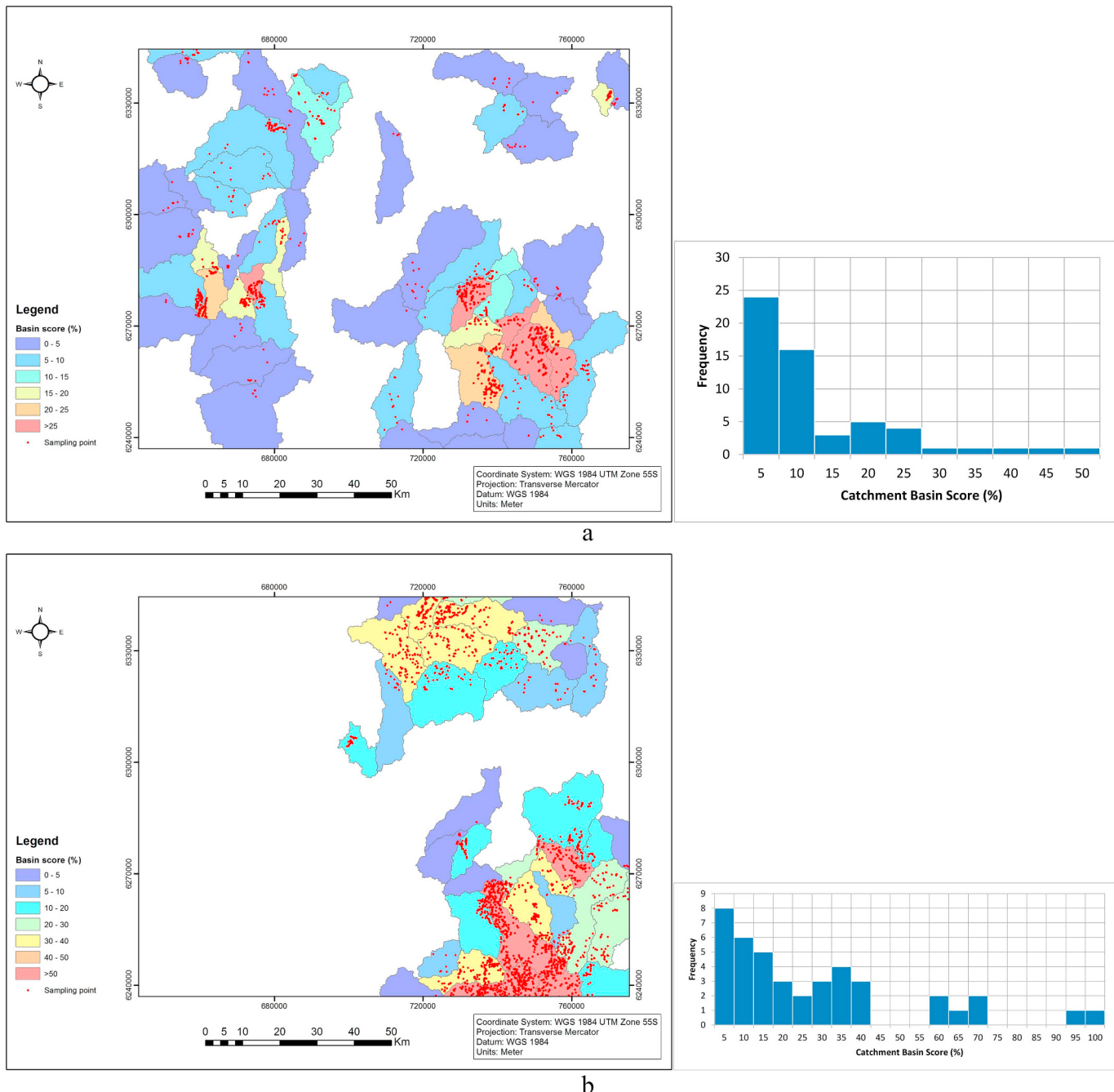


**Fig. 7.** Stream sediment samples draped over the Catchment Basin Score (CBS) map of dataset a) A, b) B and c) C, along with the corresponding histogram of CBS values.

commonly applied to assess if a distribution follows a normal distribution and also to determine the number of populations in a specific dataset (Cheng et al., 1994; Xiao et al., 2012; Zhao et al., 2016; Zuo, 2011). According to our Q-Q plots and reference lines in Fig. 9, the distributions are close to a normal distribution and the deviations from the reference lines in low and high values imply on the presence of more than one population in each dataset. Anomalous low and high values can also be interpreted as the depletion and enrichment of the relevant element in some samples. This suggests that the study area has been influenced by several geological events and mineralization processes (Reimann et al., 2002; Zuo, 2011; Zuo et al., 2009).

In the following, results of applying factor analysis on datasets A, B and C are presented, respectively. According to Table 1, dataset A involves concentration values of As, Au, Cu, Pb and Zn for 1559 samples.

After applying factor analysis, there are three output components with an eigenvalue greater than one and ~90% of the total variance of the input data is preserved in the output components. The rotated component matrix is presented in Table 4. The relationship of each variable to the underlying factor is expressed by the so-called loading values. The absolute threshold value which is usually considered to separate high from low loading values in rotated component matrix is 0.6 (e.g., Yousefi et al., 2012). Given this threshold and according to Table 4, the first component shows high absolute loading values for Au and Zn. Moreover, the second component shows high absolute loading values for Cu and Pb and the third component shows a high loading value for As. The opposite signs of Au–Zn and Cu–Pb loadings show that they are negatively correlated in corresponding factors or components. This shows that in the case when one of the elements of each association

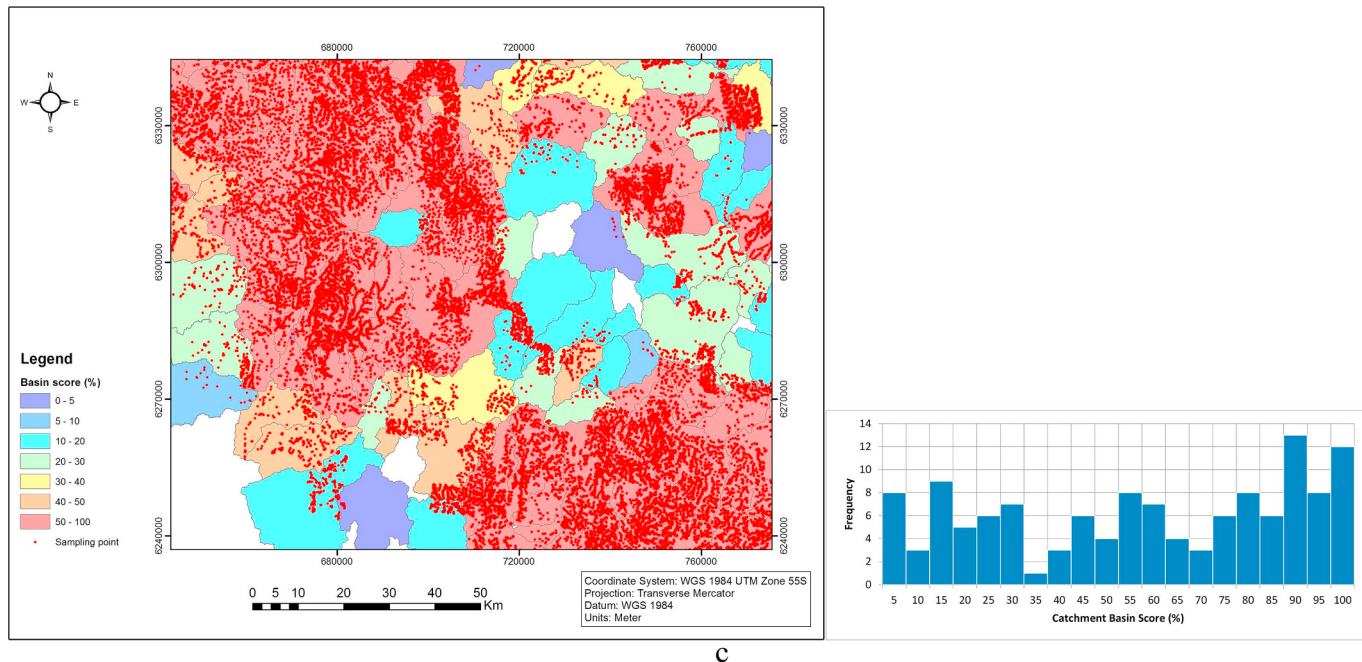


Fig. 7. (continued)

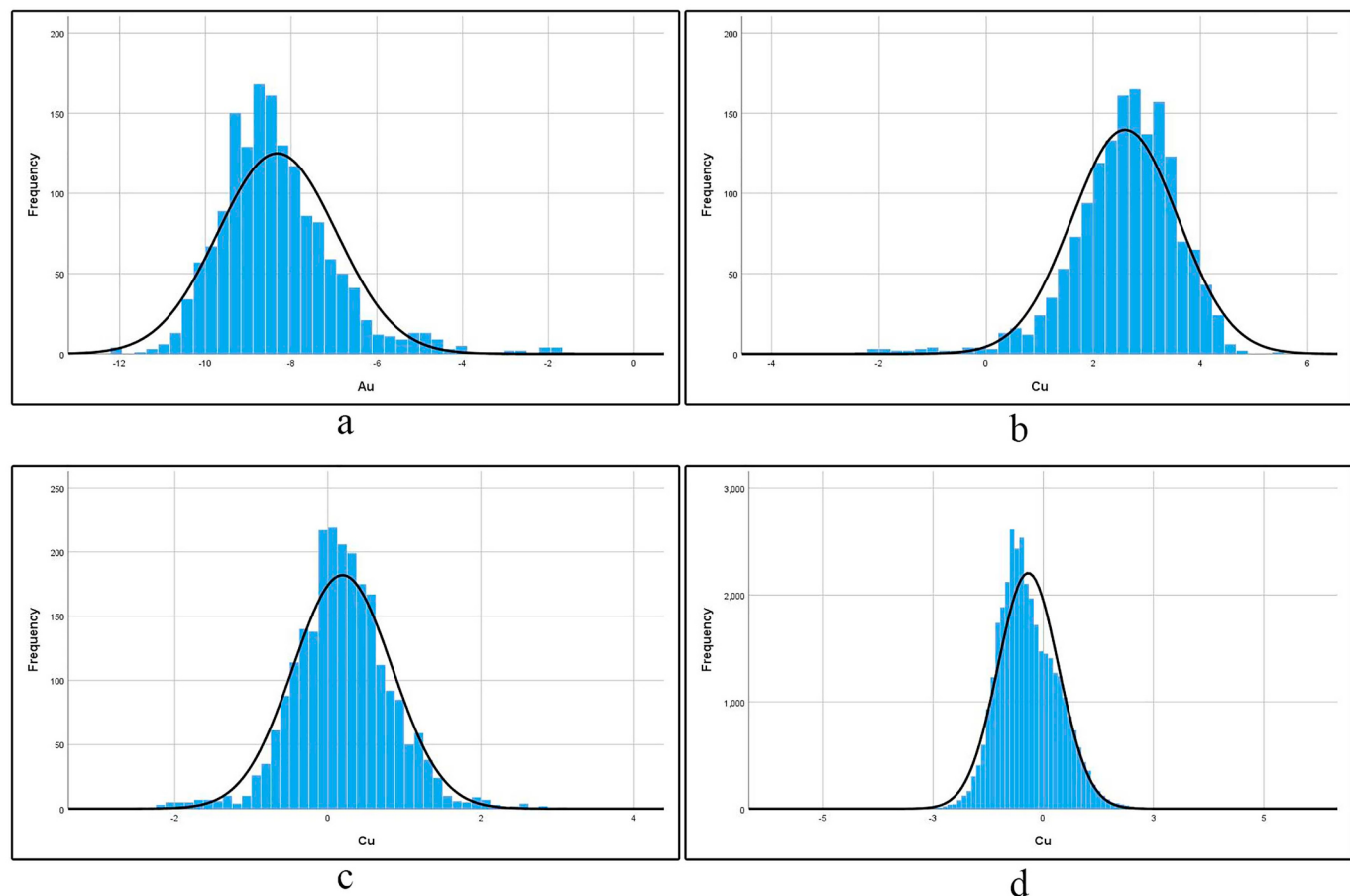
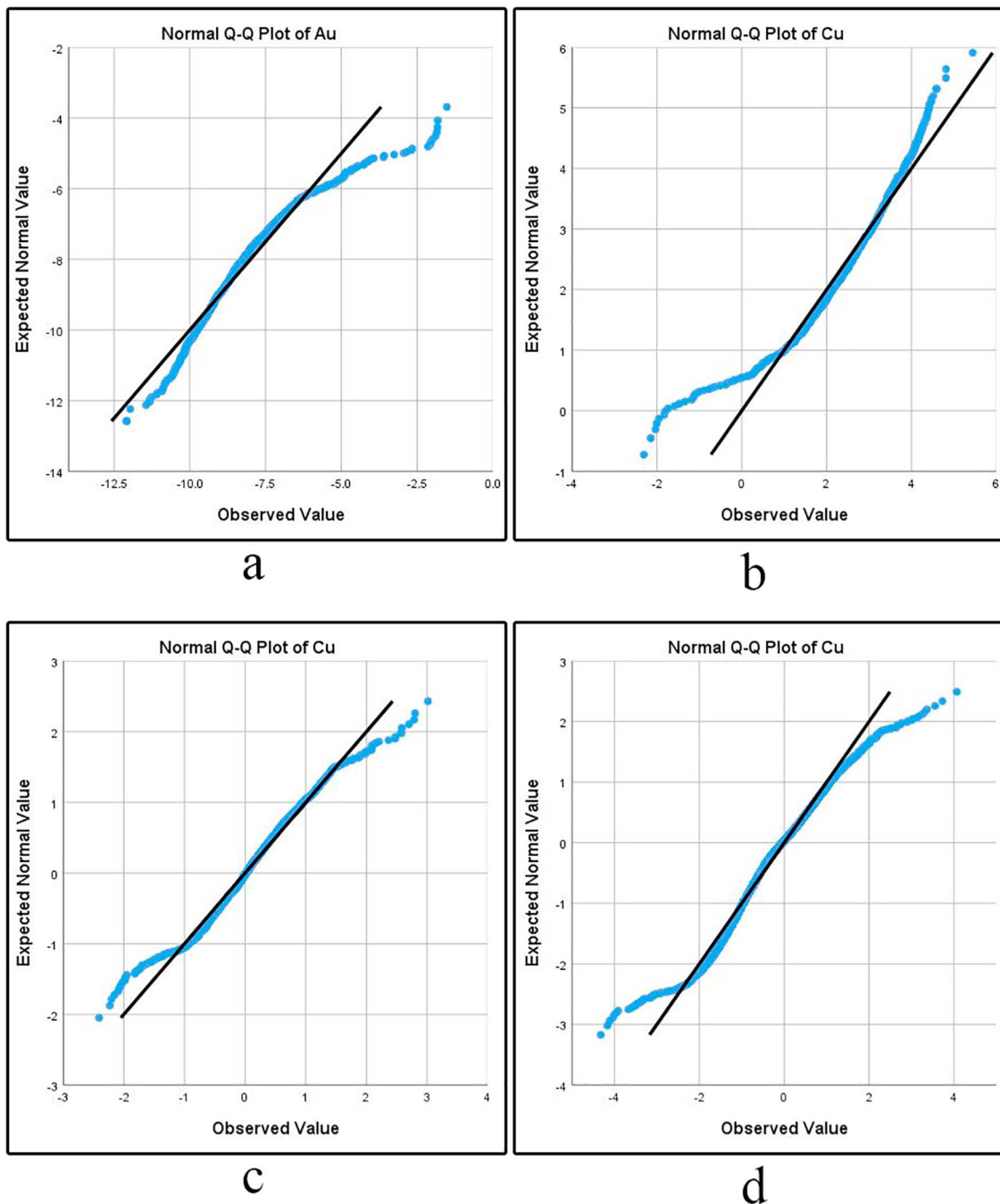


Fig. 8. Histograms of the ilr-transformed Au and Cu concentration values from dataset A are respectively shown in a and b. Histograms of the ilr-transformed Cu concentration values from datasets B and C are respectively shown in c and d.

shows high concentration values, the other shows low concentration values. In other words, enrichment of each element is associated with the depletion of the others. Since the potential areas of the porphyry

Cu–Au mineralization are the target and, Au and Cu loading values are positive in the first and second components, respectively; the corresponding factor scores are kept without any changes. Therefore, high



**Fig. 9.** Q-Q plots of the ilr-transformed Au and Cu concentration values from dataset A are respectively shown in a and b. Q-Q plots of the ilr-transformed Cu concentration values from datasets B and C are respectively shown in c and d.

factor scores in the first and second components are considered as the potential areas of the Au and Cu mineralization, respectively. However, high negative factor scores in the first and second components can be considered for prospecting high potential areas of Zn and Pb mineralization, respectively. High positive factor scores of the third component can also be used to detect high potential areas of As mineralization.

As presented in Table 1, dataset B involves concentration values of As, Co, Cu, Ni, Pb and Zn for 2359 samples. The factor analysis, yields three output components with an eigenvalue greater than one, and ~73% of the total variance of the input data is preserved in the output components. The rotated component matrix is presented in Table 5.

Considering a threshold equal of 0.6, the first component shows high loading values for Co and Ni; the second component shows high absolute loading values for As and Pb and finally, the third component shows high absolute loading values for Cu and Zn. The opposite signs of As–Pb and Cu–Zn loadings shows negative correlation in the corresponding factors or components. Concentration values of Au are ignored in this analysis due to low number of samples, thus only the third factor can be considered highly relevant to the potential areas of the Cu–Au porphyry mineralization. Note this is because the Cu loading has a high positive value. High positive factor scores in the first component can be applied to prospect high potential areas of Co–Ni mineralization. Moreover, high negative factor scores in the second

**Table 4**

Rotated component matrix which has been resulted by applying factor analysis on dataset A. Loadings in bold show anomalous values based on the absolute threshold value of 0.6.

	Component		
	F1	F2	F3
As	0.015	−0.151	<b>0.950</b>
Au	<b>0.888</b>	−0.248	−0.371
Cu	0.185	<b>0.958</b>	−0.123
Pb	0.451	<b>−0.626</b>	−0.105
Zn	−0.834	0.019	−0.197
Eigen-value	1.942	1.383	1.188
Variance (%)	38.833	27.651	23.751
Cumulative variance (%)	38.833	66.484	90.235

**Table 5**

Rotated component matrix which has been resulted by applying factor analysis on dataset B. Loadings in bold show anomalous values based on the absolute threshold value of 0.6.

	Component		
	F1	F2	F3
As	−0.426	<b>−0.904</b>	−0.102
Co	<b>0.775</b>	−0.019	−0.192
Cu	−0.127	0.225	<b>0.913</b>
Ni	<b>0.815</b>	0.140	0.055
Pb	−0.425	<b>0.687</b>	−0.217
Zn	−0.026	0.208	<b>−0.670</b>
Eigen-value	1.780	1.426	1.182
Variance (%)	29.669	23.773	19.703
Cumulative variance (%)	29.669	53.442	73.145

**Table 6**

Rotated component matrix which has been resulted by applying factor analysis on dataset C. Loadings in bold show anomalous values based on the absolute threshold value of 0.6.

	Component	
	F1	F2
Cu	<b>0.904</b>	−0.368
Pb	<b>0.981</b>	−0.275
Zn	−0.012	<b>0.995</b>
Eigen-value	1.813	1.167
Variance (%)	60.434	38.900
Cumulative variance (%)	60.343	99.243

component can lead to the high potential areas of As mineralization and, high negative factor scores in the third factor can be used to detect high potential areas of Zn mineralization.

As mentioned in Table 1, dataset C involves concentration values of Cu, Pb and Zn for 34,815 samples. After applying factor analysis, the number of output components with an eigenvalue greater than one, equals two and ~99% of the total variance of the input data is preserved in the output components. This significant value implies that the selected output components can efficiently represent concentration values of the analyzed elements. The rotated component matrix is presented in Table 6. Considering a threshold of 0.6, the first component shows high loading values for Cu and Pb, and the second component shows high loading value for Zn. Compared to the previous datasets, concentration values of As, Co and Ni are ignored due to low number of samples. The first factor can be considered highly relevant to the potential areas of the Cu–Au porphyry mineralization since the Cu loading is a high positive value. Moreover, high positive factor scores in the second component can be applied for prospecting high potential areas of Zn mineralization.

Different associations of Au and Cu are observed with the other elements which can be due to diversity of contributing elements in factor analysis and number of samples. This shows that different datasets from a same area may result in showing different associations of the elements. In the following section, the outputs of factor analysis on every three datasets are mapped using E-WDCB method.

#### 4.3. Discrete geochemical evidential layer

The factor scores of the first and second components resulting from the factor analysis on dataset A are used as the indicator of Au and Cu mineralization. Also, the factor scores of the third and first components resulting from the factor analysis on dataset B and C are used as the other indicators of Cu mineralization. The weighted catchment basins using E-WDCB method based on the Au and Cu factor scores generated by the factor analysis on dataset A, B and C are shown in Fig. 10 along with the corresponding histograms. The histograms reveal that anomalous catchment basins are well separated from the background.

Three Cu E-WDCB maps which have been presented in Fig. 10 are integrated using Eq. (6) and calculated CBSs which are shown in Fig. 7. The integrated WDCB map of Cu is shown in Fig. 11.

The map shown in Fig. 11 can be integrated with the WDCB map of Au to provide a discrete geochemical evidential layer for Cu–Au mineralization. The fuzzy gamma operator with a gamma parameter of 0.9 is used to integrate these two maps (Yousefi et al., 2013). The integrated map along with the known porphyry Cu–Au occurrences are shown in Fig. 12. It is noteworthy that the map shown in this figure involves the catchment basins which have been assigned a weight in both input maps.

The results are further compared to a canonical method, i.e. the median of factor scores. Therefore, separate maps are created for potential areas of Au and Cu mineralization by determining the median of factor scores in each catchment basin. This canonical method has been programmed using a MATLAB script which is available online.<sup>6</sup> The factor scores are separately transformed to fuzzy space in each catchment basin using Eq. (3) and then, the median has been determined. Similar to the procedure explained above, an integrated map is created using three Cu score maps and CBSs. The Au and Cu maps are integrated using the fuzzy gamma operator with a gamma parameter of 0.9. The result is shown in Fig. 13 along with the known porphyry Cu–Au occurrences in the study area.

In order to quantitatively validate the results obtained from different maps, the Prediction-Area (P-A) plot is used (Yousefi and Carranza, 2015b). In a P-A plot, the cumulative percentage of predicted known occurrences and their corresponding cumulative occupied areas with respect to the total area are shown in relation to the prospectivity values. Therefore, the prediction ability of a prospectivity map and its ability to delimit the study area for further exploration are evaluated in a scheme (Yousefi and Carranza, 2016).

The P-A plot shows a curve of the percentage (prediction rate) of known mineral occurrences and a curve of the percentage of occupied areas corresponding to the classes of a prospectivity map. When an intersection point of the two curves is at a higher place, it portrays a small area containing a large number of mineral deposits. Furthermore, it objectively chooses a better model to give priority for mineral exploration (Shokouh Saljoughi et al., 2018; Yousefi and Carranza, 2015a).

The comparison of the prediction rates in the P-A plots (Fig. 14) shows the importance of analyzing the predictability of prospectivity maps. Here, we have compared four discrete geochemical maps including the E-WDCB map of Au resulting from dataset A (Fig. 10a), final E-WDCB map of Cu resulting from integrating three E-WDCB maps (Fig. 11), and two integrated maps shown in Figs. 12 and 13. The

<sup>6</sup> <https://github.com/intelligent-exploration/3S>.

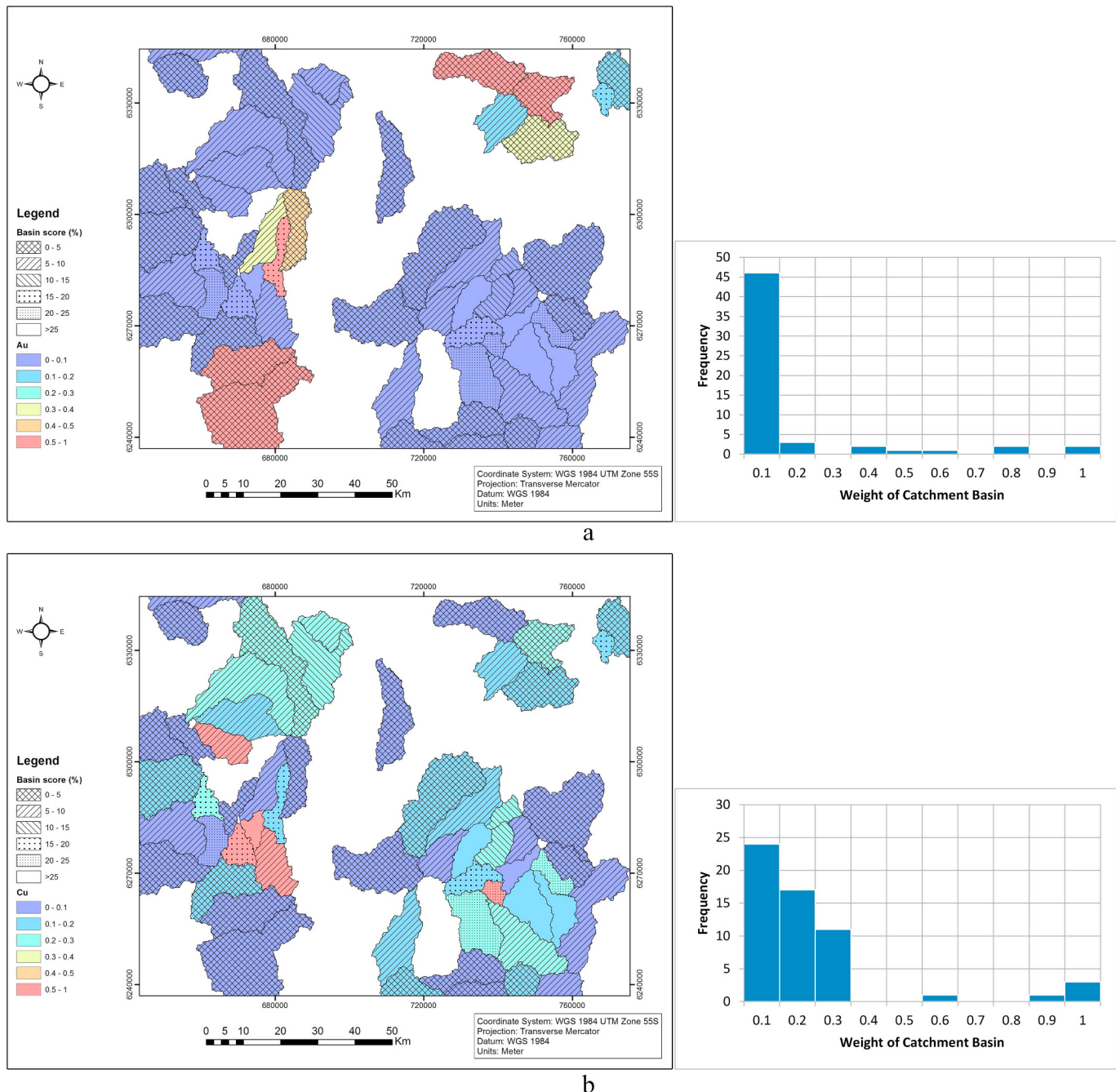


**Fig. 10.** a) Weighted catchment basins based on the Au factor scores generated by the factor analysis on dataset A along with the corresponding histogram. b, c, d) Weighted catchment basins based on the Cu factor scores generated by the factor analysis on dataset A, B and C along with the corresponding histograms.

intersection point in the P-A plot of the map from the proposed method (Fig. 14c) shows 75% of the known Cu occurrences predicted in 25% of the total study area. The intersection point in the P-A plot corresponding to the applied canonical method shows 65% of the known Cu occurrences predicted in 35% of the total study area. The attributes of the intersection points in the P-A plots are shown in Table 7. The comparison of the presented data demonstrates a higher efficiency of the discrete geochemical map obtained using the proposed method for prospecting porphyry Cu–Au mineralization.

## 5. Discussion

We investigated the efficiency of an enhanced method for discrete geochemical mapping of the stream sediment anomalies. Stream

sediment samples are irregularly scattered in the study area and thus continuous mapping is challenging and sometimes causes neglecting locally high values (Zuo, 2011). Factor analysis was applied to three datasets with different elements and sampling points. The association of the elements with Cu changes in each dataset by increasing the number of sampling points and changes in contributing elements. Pb shows a high negative correlation with Cu according to the outputs of factor analysis on dataset A. This correlation changes to near zero according to the outputs of factor analysis on dataset B. The Cu shows high positive and negative correlation with Pb and Zn according to the results of factor analysis on dataset C. We note that dataset C has the maximum number of sampling points. Dataset C can be more reliable due to much higher number of samples compared to the other two datasets and thus the association of Cu–Pb can be used as a robust indicator of Cu

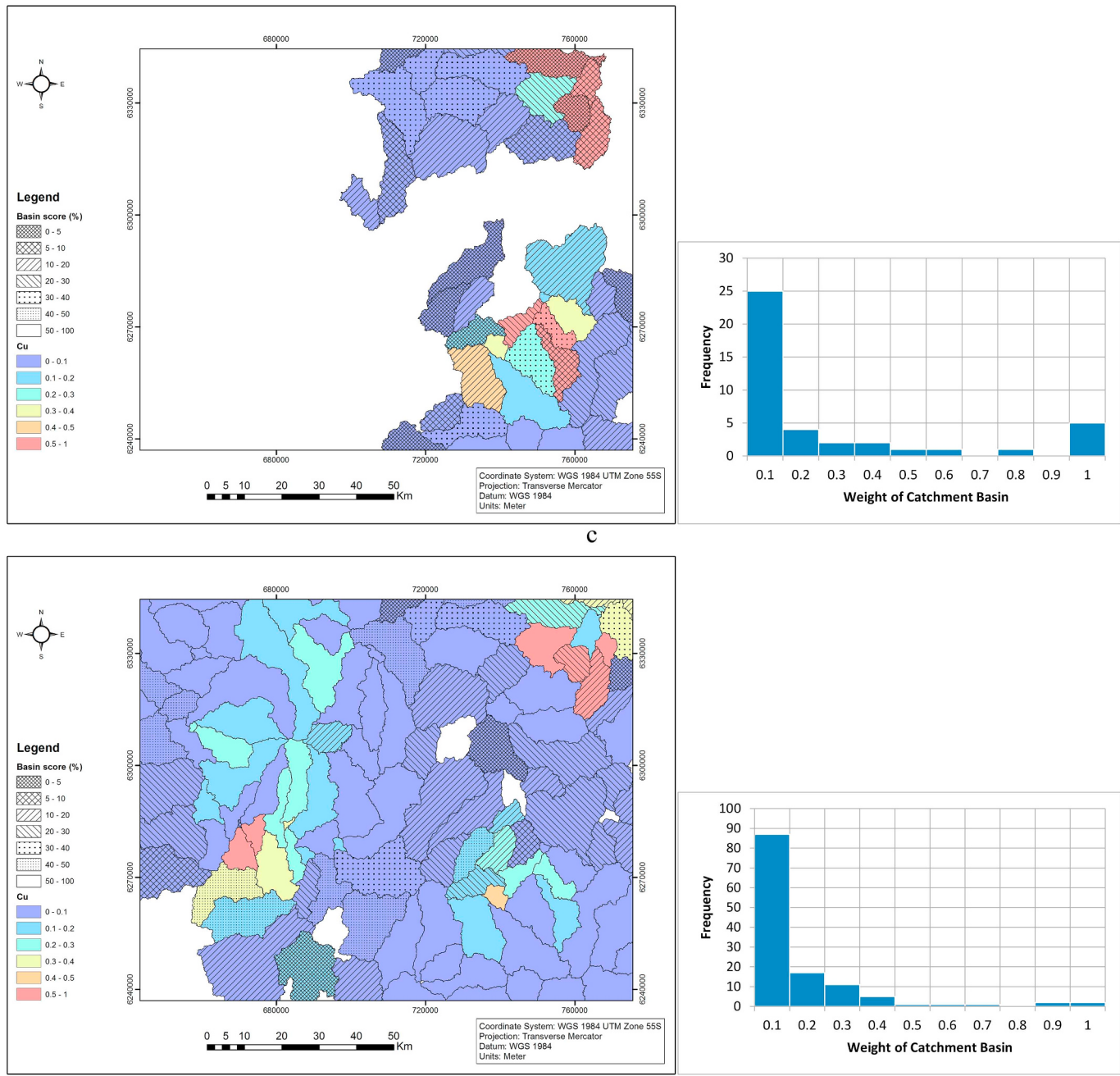


Fig. 10. (continued)

mineralization in the study area. According to the output of factor analysis on dataset A, we observed that Au is negatively correlated with Zn. We note that dataset A is the only dataset involving Au concentration value.

Geochemical mapping using the stream sediment samples is challenging in general, because extracted anomalies are not always spatially coincident with indicative geological features such as intrusive bodies (Spadoni et al., 2004). Stream sediment samples originate from transported materials, while geological features are in situ and this makes geochemical mapping challenging. Thus, in regions with complex geochemical patterns, some mineralized areas may be missed (Carranza, 2011; Pazand et al., 2011; Ranasinghe et al., 2008; Yousefi et al., 2012; Zuo, 2011; Zuo et al., 2009). This can also happen due to inefficiency of the geochemical mapping techniques to consider all of the aspects of sediment transport processes involved. This suggests that

elements with different physical and chemical characteristics such as mobility may show anomalies in different locations downstream from an anomaly source such as an ore body (Xie et al., 2010; Yilmaz, 2003; Yousefi et al., 2012). Therefore, considering catchment basins and weighting according to the geochemical characteristics shown by the stream sediment samples can lead to accurate detection of anomaly patterns.

We developed the E-WDCB method to detect anomalous catchment basins which can be applied to one or several geochemical indicators such as concentration values. In this study, factor scores resulting from the factor analysis on different sets of elements are used as the geochemical indicators (Fig. 10). The E-WDCB MATLAB code which is freely available online, makes it possible to use different sets of thresholds for separating anomalous samples from the background. This method can be combined with anomaly-background separation

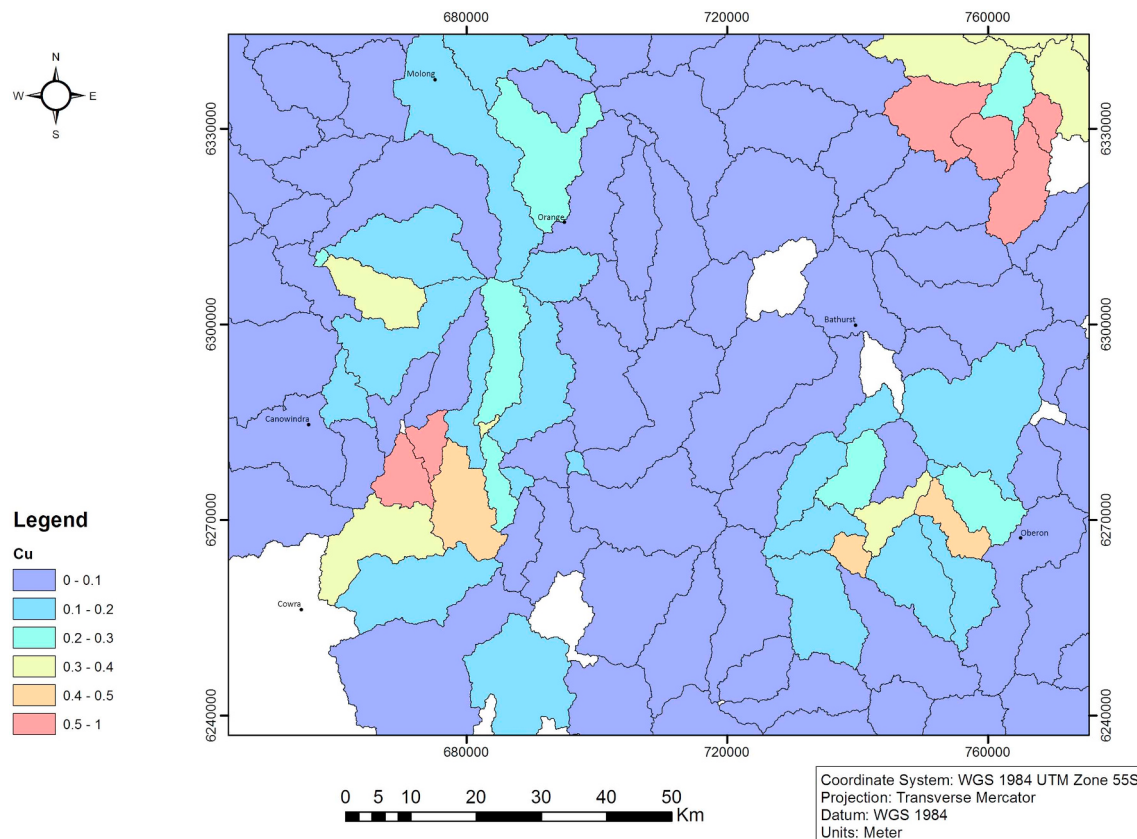


Fig. 11. Integrated E-WDCB map of Cu which is the result of integrating three datasets using CBSs.

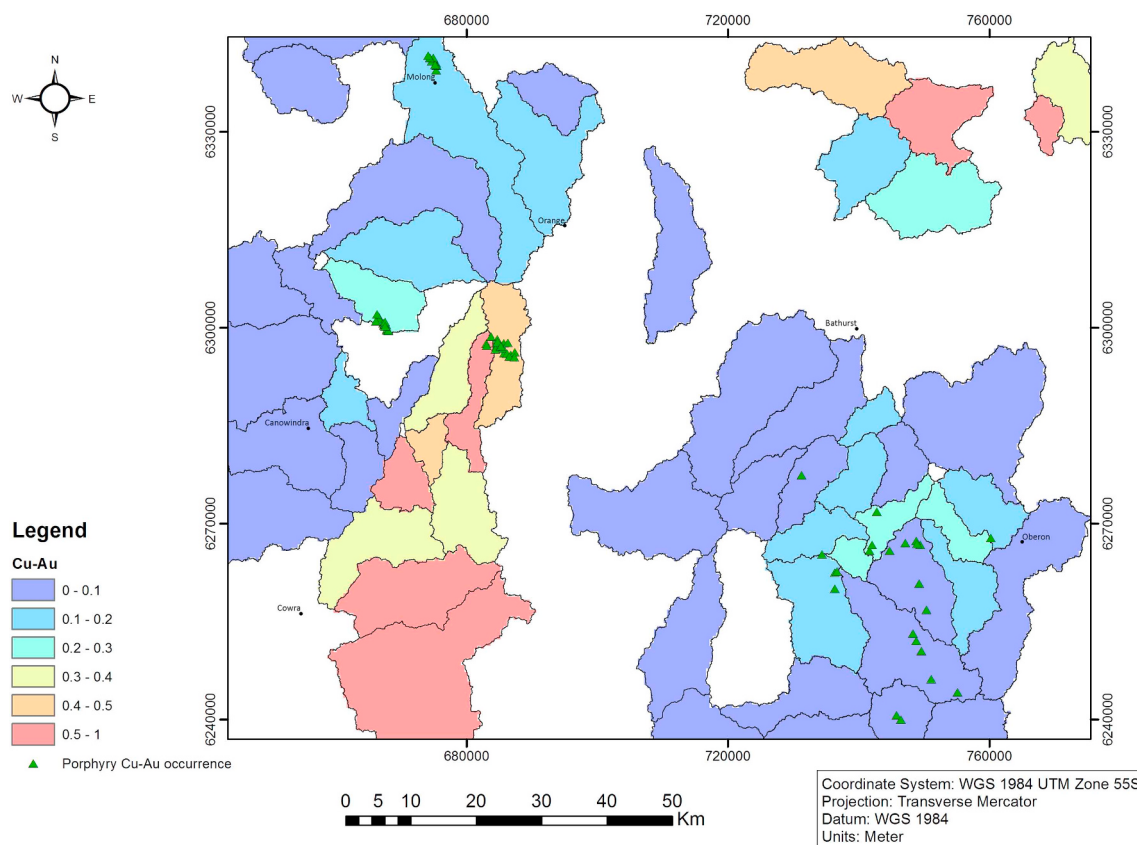
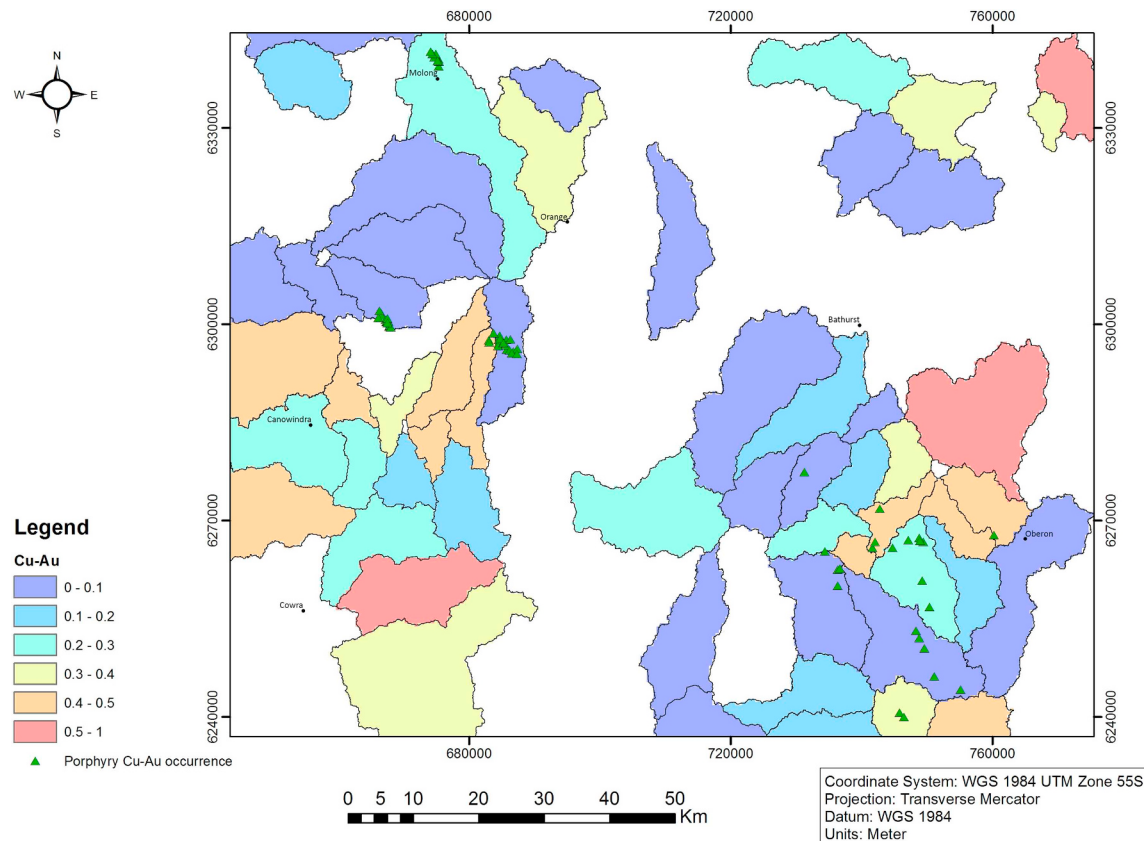
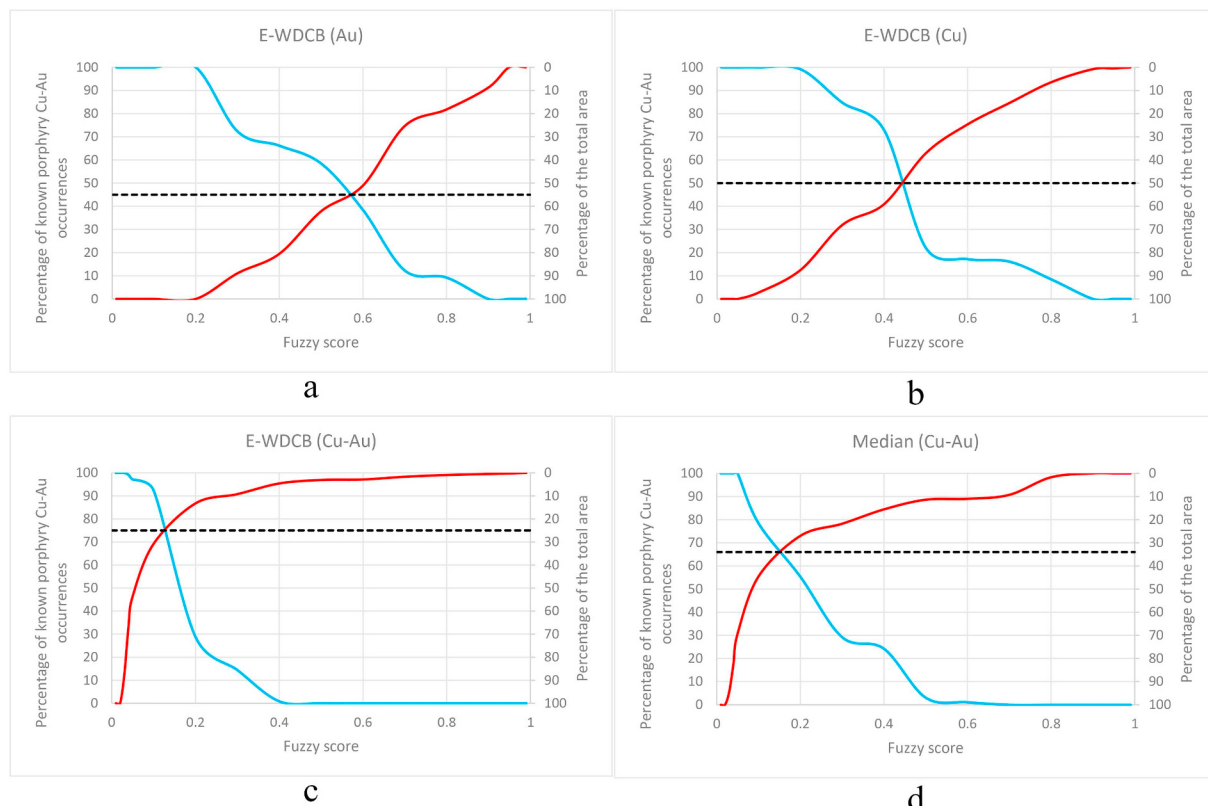


Fig. 12. Superposition of known porphyry Cu–Au mineral occurrences on the integrated map using E-WDCB maps of Au and Cu showing potential catchment basins.



**Fig. 13.** Superposition of known porphyry Cu–Au occurrences on the fuzzy integrated map provided by the median of factor scores resulting from Au and Cu indicator components.

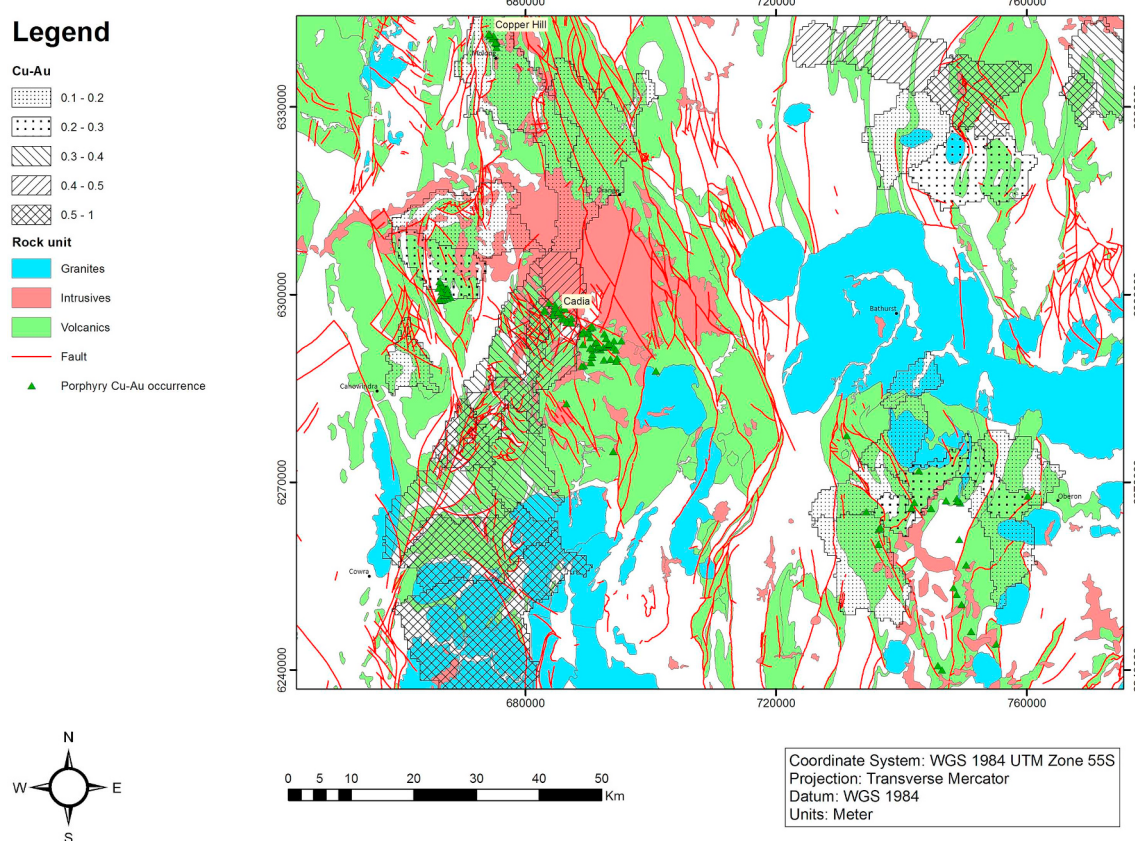


**Fig. 14.** P-A plots for discrete geochemical maps generated by E-WDCB method for a) Au, b) Cu, c) Cu and Au, and d) median of Cu and Au factor scores.

**Table 7**

Attributes of the intersection points obtained from the P-A plots.

Discrete geochemical map	Prediction rate (%)	Occupied area (%)
WDCB (Au)	45	55
WDCB (Cu)	50	50
WDCB (Cu–Au)	75	25
Median (Cu–Au)	65	35

**Fig. 15.** Anomalous catchment basins draped over the classified geological map of the study area.

methods such as fractal methods. The proposed CBS index can be used to evaluate suitability of sampling points in a catchment basin and to integrate different discrete geochemical maps. The CBS index can also be used to determine to what extent the samples within a catchment basin can represent specific geochemical characteristics such as concentration value of an element. We used this index to integrate three discrete geochemical maps of Cu mineralization resulting from applying E-WDCB method on different datasets (Fig. 11).

One of the critical aspects of mineral prospecting and understanding ore geometry is to recognize the association between geochemical anomalies and geological features (Wang et al., 2013; Ziai et al., 2011). The map shown in Fig. 12 has been draped over the geological map of the study area which is available in Fig. 15. The geological map in this figure has been classified to granites, intrusives and volcanics. According to this figure and Fig. 2, most of the anomalous catchment basins are well correlated with the Ordovician volcanic rocks and Cainozoic mafic volcanics. Also, Silurian I-type and I-S trans-type granites located east of Cowra show significant correlation with anomalous catchment basins in south western section of the study area (Figs. 2 and 15). These catchment basins show a low CBS (Fig. 7) which makes the weight determined for them relatively unreliable but further exploration operations in this area and also North Eastern section of the study area are highly recommended due to low number of sampling

points and high probability of mineralization. Cadia and Copper Hill mines as two well-known porphyry Cu–Au occurrences in the study area, located in the catchment basins which are mostly covered by the volcanics and partly intrusives, and their catchment basins are weighted higher than the background. It should be pointed that anomalous catchment basins including a high number of porphyry Cu–Au occurrences are well correlated with lineaments such as faults (Fig. 15) which play an important role in the genesis of the porphyry

systems (Sillitoe, 2010).

## 6. Conclusions

In this study, we provide a discrete geochemical map of anomalies using the results of analyzing stream sediment samples collected within the Bathurst 1:250K map sheet, New South Wales, Australia. The diversity of data sources from which the results of analyzing stream sediment samples can be accessed makes analyzing and interpreting the data more complicated. In some cases, the samples are scattered non-uniformly and thus the sampling density is highly variable throughout the study area. Our findings show that applying discrete mapping such as the E-WDCB method is more reliable when compared to canonical methods for mapping the geochemically anomalous catchment basins. Three different datasets were analyzed by applying factor analysis as a well-known multivariate analysis to create different components for each dataset. According to the results, we observe that the output can be highly dependent on the number of sampling points and contributing elements.

The proposed Catchment Basin Score is an index to delineate the suitability of sampling in a catchment basin. It can also be used to integrate the output components into one for each element of the samples. We observed that the final discrete geochemical map of Cu and Au

created by integrating E-WDCB maps of these two elements shows a higher prediction rate when compared to maps created by canonical methods. The anomalous catchment basins in this map are well correlated with known porphyry Cu–Au occurrences and they are mostly coincident with Ordovician volcanic rocks and Cainozoic mafic volcanics. Moreover, Silurian I-type and I–S trans-type granites show significant correlation with anomalous catchment basins in the east of Cowra. The low number of sampling points in South Western and North Eastern sections of the study area which show high probability of mineralization shows the necessity of further exploration operations in these areas.

In future work, the proposed methods can be applied for creating an efficient discrete geochemical map using stream sediment samples in a regional scale and even it can be improved further by applying fractal methods. Since discrete maps show stronger positive spatial associations with known mineral occurrences compared to continuous maps, they can be used as more reliable evidential layers for mineral prospectivity mapping.

## Acknowledgments

The authors would like to thank Prof. E. J. M. Carranza for handling this paper. We express our gratitude to Dr. M. Yousefi for his constructive comments. We also appreciate other anonymous reviewers for their valuable comments which helped to improve this paper.

## References

- Agterberg, F.P., 1992. Combining indicator patterns in weights of evidence modeling for resource evaluation. *Nonrenewable Resour.* 1, 39–50. <https://doi.org/10.1007/BF01782111>.
- Agterberg, F.P., Bonham-Carter, G.F., 2005. Measuring the performance of mineral-potential maps. *Nat. Resour. Res.* 14, 1–17. <https://doi.org/10.1007/s11053-005-4674-0>.
- Aitchison, J., 1986. *The Statistical Analysis of Compositional Data*. The Blackburn Press.
- Aitchison, J., Egoscue, J.J., 2005. Compositional data analysis: where are we and where should we be heading? *Math. Geol.* 37, 829–850. <https://doi.org/10.1007/s11004-005-7383-7>.
- Bai, J., Porwal, A., Hart, C., Ford, A., Yu, L., 2010. Mapping geochemical singularity using multifractal analysis: application to anomaly definition on stream sediments data from Funin Sheet, Yunnan, China. *J. Geochem. Explor.* 104, 1–11. <https://doi.org/10.1016/j.gexplo.2009.09.002>.
- Bogen, J., Bolvikken, B., Otesen, R.T., 1992. Environmental studies in Western Europe using overbank sediment. In: *Erosion and Sediment Monitoring Programmes in River Basins*. International Association of Hydrological Sciences Publication, pp. 317–325.
- Bonham-Carter, G.F., 1994. *Geographic Information Systems for Geoscientists*. Elsevier.
- Bonham-Carter, G.F., Goodfellow, W.D., 1986. Background corrections to stream geochemical data using digitized drainage and geological maps: application to Selwyn Basin, Yukon and Northwest Territories. *J. Geochem. Explor.* 25, 139–155. [https://doi.org/10.1016/0375-6742\(86\)90011-7](https://doi.org/10.1016/0375-6742(86)90011-7).
- Bonham-Carter, G.F., Goodfellow, W.D., 1984. Autocorrelation structure of stream-sediment geochemical data: interpretation of Zn and Pb anomalies, Nahanni River area, Yukon-Northwest Territories, Canada. *Geostatistics Nat. Resour. Charact.* 2, 817–829.
- Bookstrom, A.A., Len, R.A., Hammarstrom, J.M., Robinson Jr., Gilpin, R., Zientek, M.L., Drenth, B.J., Jaireth, S., Cossette, P.M., Wallis, J.C., 2014. Porphyry copper assessment of eastern Australia: chapter L in global mineral resource assessment. Scientific Investigations Report. <https://doi.org/10.3133/sir20105090L>.
- Buccianti, A., 2015. The FOREGS repository: modelling variability in stream water on a continental scale revising classical diagrams from CoDA (compositional data analysis) perspective. *J. Geochem. Explor.* 154, 94–104. <https://doi.org/10.1016/j.gexplo.2014.12.003>.
- Buccianti, A., Grunsky, E., 2014. Compositional data analysis in geochemistry: are we sure to see what really occurs during natural processes? *J. Geochem. Explor.* 141, 1–5. <https://doi.org/10.1016/j.gexplo.2014.03.022>.
- Carranza, E.J.M., 2015. Data-driven evidential belief modeling of mineral potential using few prospects and evidence with missing values. *Nat. Resour. Res.* 24, 291–304. <https://doi.org/10.1007/s11053-014-9250-z>.
- Carranza, E.J.M., 2011. Analysis and mapping of geochemical anomalies using logratio-transformed stream sediment data with censored values. *J. Geochem. Explor.* 110, 167–185. <https://doi.org/10.1016/j.gexplo.2011.05.007>.
- Carranza, E.J.M., 2010. Mapping of anomalies in continuous and discrete fields of stream sediment geochemical landscapes. *Geochemistry Explor. Environ. Anal.* 10, 171–187. <https://doi.org/10.1144/1467-7873/09-223>.
- Carranza, E.J.M., 2008. *Geochemical Anomaly and Mineral Prospectivity Mapping in GIS*. Elsevier.
- Carranza, E.J.M., 2004. Usefulness of stream order to detect stream sediment geochemical anomalies. *Geochemistry Explor. Environ. Anal.* 4, 341–352. <https://doi.org/10.1144/1467-7873/03-040>.
- Carranza, E.J.M., Hale, M., 1997. A catchment basin approach to the analysis of reconnaissance geochemical-geological data from Albay Province, Philippines. *J. Geochem. Explor.* 60, 157–171. [https://doi.org/10.1016/S0375-6742\(97\)00032-0](https://doi.org/10.1016/S0375-6742(97)00032-0).
- Carranza, E.J.M., Laborte, A.G., 2015a. Random forest predictive modeling of mineral prospectivity with small number of prospects and data with missing values in Abra (Philippines). *Comput. Geosci.* 74, 60–70. <https://doi.org/10.1016/j.cageo.2014.10.004>.
- Carranza, E.J.M., Laborte, A.G., 2015b. Data-driven predictive mapping of gold prospectivity, Baguio district, Philippines: application of Random Forests algorithm. *Ore Geol. Rev.* 71, 777–787. <https://doi.org/10.1016/j.oregeorev.2014.08.010>.
- Cheng, Q., 2007. Mapping singularities with stream sediment geochemical data for prediction of undiscovered mineral deposits in Gejiu, Yunnan Province, China. *Ore Geol. Rev.* 32, 314–324. <https://doi.org/10.1016/j.oregeorev.2006.10.002>.
- Cheng, Q., Agterberg, F.P., Ballantyne, S.B., 1994. The separation of geochemical anomalies from background by fractal methods. *J. Geochem. Explor.* 51, 109–130. [https://doi.org/10.1016/0375-6742\(94\)90013-2](https://doi.org/10.1016/0375-6742(94)90013-2).
- Chivas, A.R., Nutter, A.H., 1975. Copper Hill porphyry-copper prospect. *Econ. Geol. Aust. Papua New Guinea* 1, 716–720.
- Cooke, D.R., Wilson, A.J., House, M.J., Wolfe, R.C., Walshe, J.L., Lickfold, V., Crawford, A.J., 2007. Alkalic porphyry Au–Cu and associated mineral deposits of the Ordovician to Early Silurian Macquarie Arc, New South Wales. *Aust. J. Earth Sci.* 54, 445–463. <https://doi.org/10.1080/08120090601146771>.
- Degeling, P.R., Gilligan, L.B., Scheibner, E., Suppel, D.W., 1986. Metallogeny and tectonic development of the Tasman Fold Belt System in New South Wales. *Ore Geol. Rev.* 1, 259–313. [https://doi.org/10.1016/0169-1368\(86\)90011-9](https://doi.org/10.1016/0169-1368(86)90011-9).
- Egoscue, J.J., Pawłowsky-Glahn, V., Mateu-Figueras, G., Barceló-Vidal, C., 2003. Isometric logratio transformations for compositional data analysis. *Math. Geol.* 35, 279–300. <https://doi.org/10.1023/A:1023818214614>.
- El-Makky, A.M., 2011. Statistical analyses of La, Ce, Nd, Y, Nb, Ti, P, and Zr in bedrocks and their significance in geochemical exploration at the Um Garayat Gold Mine Area, Eastern Desert, Egypt. *Nat. Resour. Res.* 20, 157–176. <https://doi.org/10.1007/s11053-011-9144-2>.
- El-Makky, A.M., Sediek, K.N., 2012. Stream sediments geochemical exploration in the northwestern part of Wadi Allaqa Area, South Eastern Desert, Egypt. *Nat. Resour. Res.* 21, 95–115. <https://doi.org/10.1007/s11053-011-9166-9>.
- Farahbakhsh, E., Shirmand, H., Bahroudi, A., Eslamkash, T., 2016. Fusing ASTER and QuickBird-2 satellite data for detailed investigation of porphyry copper deposits using PCA: case study of Naysian deposit, Iran. *J. Indian Soc. Remote Sens.* 44, 525–537. <https://doi.org/10.1007/s12524-015-0516-7>.
- Filzmoser, P., Hron, K., Reimann, C., 2009a. Univariate statistical analysis of environmental (compositional) data: problems and possibilities. *Sci. Total Environ.* 407, 6100–6108. <https://doi.org/10.1016/j.scitotenv.2009.08.008>.
- Filzmoser, P., Hron, K., Reimann, C., 2009b. Principal component analysis for compositional data with outliers. *Environmetrics* 20, 621–632. <https://doi.org/10.1002/env.966>.
- Filzmoser, P., Hron, K., Reimann, C., Garrett, R., 2009c. Robust factor analysis for compositional data. *Comput. Geosci.* 35, 1854–1861. <https://doi.org/10.1016/j.cageo.2008.12.005>.
- Gilligan, L.B., Markham, N.L., Suppel, D.W., 1976. *Ore Deposits of the Lachlan Fold Belt, New South Wales*. International Geological Congress.
- Glen, R.A., Crawford, A.J., Cooke, D.R., 2007. Tectonic setting of porphyry Cu–Au mineralisation in the Ordovician–Early Silurian Macquarie Arc, Eastern Lachlan Orogen, New South Wales. *Aust. J. Earth Sci.* 54, 465–479. <https://doi.org/10.1080/0812009070121672>.
- Glen, R.A., Saeed, A., Quinn, C.D., Griffin, W.L., 2011. U–Pb and Hf isotope data from zircons in the Macquarie Arc, Lachlan Orogen: implications for arc evolution and Ordovician palaeogeography along part of the East Gondwana margin. *Gondwana Res.* 19, 670–685. <https://doi.org/10.1016/j.gr.2010.11.011>.
- Gray, D.R., 1997. Tectonics of the southeastern Australian Lachlan Fold Belt: structural and thermal aspects. *Geol. Soc. Lond. Spec. Publ.* 121, 149 LP–177. <https://doi.org/10.1144/GSL.SP.1997.121.01.07>.
- Gulson, B.L., Bofiger, V.M., 1972. Time differences within a calc-alkaline association. *Contrib. Mineral. Petrol.* 36, 19–26. <https://doi.org/10.1007/BF00372831>.
- He, F., ping, Wang, Z., Fang, C., Wang, L., Geng, X., 2014. Identification and assessment of Sn-polymetallic prospects in the Gejiu western district, Yunnan (China). *J. Geochem. Explor.* 145, 106–113. <https://doi.org/10.1016/j.gexplo.2014.05.016>.
- He, J., Yao, S., Zhang, Z., You, G., 2013. Complexity and productivity differentiation models of metallogenetic indicator elements in rocks and supergene media around Daijiazhuang Pb–Zn deposit in Dangchang County, Gansu province. *Nat. Resour. Res.* 22, 19–36. <https://doi.org/10.1007/s11053-012-9193-1>.
- Holliday, J.R., Wilson, A.J., Blevin, P.L., Tedder, I.J., Dunham, P.D., Pfitzner, M., 2002. Porphyry gold–copper mineralisation in the Cadia district, Eastern Lachlan Fold Belt, New South Wales, and its relationship to shoshonitic magmatism. *Miner. Depos.* 37, 100–116. <https://doi.org/10.1007/s00126-001-0233-8>.
- Howarth, R.J., Thornton, I., 1983. Regional geochemical mapping and its application to environmental studies. In: *Applied Environmental Geochemistry*. Academic Press, pp. 41–73.
- Johnson, R.A., Wichern, D.W., 2007. *Applied Multivariate Statistical Analysis*, 6th ed. Pearson.
- Kaiser, H.F., 1958. The varimax criterion for analytic rotation in factor analysis. *Psychometrika* 23, 187–200. <https://doi.org/10.1007/BF02289233>.
- Kreuzer, O.P., Miller, A.V.M., Peters, K.J., Payne, C., Wildman, C., Partington, G.A., Puccioni, E., McMahon, M.E., Etheridge, M.A., 2015. Comparing prospectivity modelling results and past exploration data: a case study of porphyry Cu–Au mineral systems in the Macquarie Arc, Lachlan Fold Belt, New South Wales. *Ore Geol. Rev.* 71, 516–544. <https://doi.org/10.1016/j.oregeorev.2014.09.001>.
- Krumbein, W.C., Graybill, F.A., 1965. *An Introduction to Statistical Models in Geology*, 1st ed. McGraw Hill.
- Kumru, M.N., Bakaç, M., 2003. R-mode factor analysis applied to the distribution of elements in soils from the Aydin Basin, Turkey. *J. Geochem. Explor.* 77, 81–91. [https://doi.org/10.1016/S0375-6742\(02\)00271-6](https://doi.org/10.1016/S0375-6742(02)00271-6).
- Lickfold, V., Cooke, D.R., Crawford, A.J., Fanning, C.M., 2007. Shoshonitic magmatism

- and the formation of the Northparkes porphyry Cu-Au deposits, New South Wales. *Aust. J. Earth Sci.* 54, 417–444. <https://doi.org/10.1080/08120090601175754>.
- Lickfold, V., Cooke, D.R., Smith, S.G., Ullrich, T.D., 2003. Endeavour copper-gold porphyry deposits, Northparkes, New South Wales: intrusive history and fluid evolution. *Econ. Geol.* 98, 1607–1636. <https://doi.org/10.2113/gsecongeo.98.8.1607>.
- Liu, Y., Cheng, Q., Xia, Q., Wang, X., 2014. Mineral potential mapping for tungsten polymetallic deposits in the Nanling metallogenic belt, South China. *J. Earth Sci.* 25, 689–700. <https://doi.org/10.1007/s12583-014-0466-y>.
- Lusty, P.A.J., Scheib, C., Gunn, A.G., Walker, A.S.D., 2012. Reconnaissance-scale prospectivity analysis for gold mineralisation in the Southern Uplands-Down-Longford Terrane, Northern Ireland. *Nat. Resour. Res.* 21, 359–382. <https://doi.org/10.1007/s11053-012-9183-3>.
- Macklin, M.G., Ridgway, J., Passmore, D.G., Rumsby, B.T., 1994. The use of overbank sediment for geochemical mapping and contamination assessment: results from selected English and Welsh floodplains. *Appl. Geochem.* 9, 689–700. [https://doi.org/10.1016/0883-2927\(94\)90028-0](https://doi.org/10.1016/0883-2927(94)90028-0).
- Marjoribanks, R., 2010. *Geological Methods in Mineral Exploration and Mining*. Springer.
- Matějíček, L., Benešová, L., Tonika, J., 2003. Ecological modelling of nitrate pollution in small river basins by spreadsheets and GIS. *Ecol. Model.* 170, 245–263. [https://doi.org/10.1016/S0304-3800\(03\)00232-1](https://doi.org/10.1016/S0304-3800(03)00232-1).
- McA. Powell, C., 1976. Geology of hill end trough Molong high: a critical appraisal of the tectonic history of the hill end trough and its margins. *Explor. Geophys.* 7, 14–18. <https://doi.org/10.1071/EG976014>.
- Montgomery, D.C., Runger, G.C., Hubele, N.F., 2010. *Engineering Statistics*, 5th ed. John Wiley & Sons.
- Moon, C.J., 1999. Towards a quantitative model of downstream dilution of point source geochemical anomalies. *J. Geochem. Explor.* 65, 111–132. [https://doi.org/10.1016/S0375-6742\(98\)00065-X](https://doi.org/10.1016/S0375-6742(98)00065-X).
- Ohta, A., Imai, N., Terashima, S., Tachibana, Y., 2005. Influence of surface geology and mineral deposits on the spatial distributions of elemental concentrations in the stream sediments of Hokkaido, Japan. *J. Geochem. Explor.* 86, 86–103. <https://doi.org/10.1016/j.gexplo.2005.04.002>.
- Parsa, M., Maghsoudi, A., Yousefi, M., Sadeghi, M., 2016. Recognition of significant multi-element geochemical signatures of porphyry Cu deposits in Noghduz area, NW Iran. *J. Geochem. Explor.* 165, 111–124. <https://doi.org/10.1016/j.gexplo.2016.03.009>.
- Pazand, K., Hezarkhani, A., Ataei, M., Ghanbari, Y., 2011. Application of multifractal modeling technique in systematic geochemical stream sediment survey to identify copper anomalies: a case study from Ahar, Azarbaijan, Northwest Iran. *Chemie der Erde - Geochemistry* 71, 397–402. <https://doi.org/10.1016/j.chemer.2011.08.003>.
- Ranasinghe, P.N., Fernando, G.W.A.R., Dissanayake, C.B., Rupasinghe, M.S., 2008. Stream sediment geochemistry of the Upper Mahaweli River Basin of Sri Lanka-geological and environmental significance. *J. Geochem. Explor.* 99, 1–28. <https://doi.org/10.1016/j.gexplo.2008.02.001>.
- Raymond, O.L., Pogson, D.J., 1998. *Bathurst 1:250 000 Geological Sheet SI/55-08, 2nd edition*.
- Reimann, C., Filzmoser, P., 2000. Normal and lognormal data distribution in geochemistry: death of a myth. Consequences for the statistical treatment of geochemical and environmental data. *Environ. Geol.* 39, 1001–1014. <https://doi.org/10.1007/s002549900081>.
- Reimann, C., Filzmoser, P., Garrett, R.G., 2002. Factor analysis applied to regional geochemical data: problems and possibilities. *Appl. Geochem.* 17, 185–206. [https://doi.org/10.1016/S0883-2927\(01\)00066-X](https://doi.org/10.1016/S0883-2927(01)00066-X).
- Sadeghi, M., Billay, A., Carranza, E.J.M., 2015. Analysis and mapping of soil geochemical anomalies: implications for bedrock mapping and gold exploration in Giyani area, South Africa. *J. Geochem. Explor.* 154, 180–193. <https://doi.org/10.1016/j.gexplo.2014.11.018>.
- Sadeghi, M., Morris, G.A., Carranza, E.J.M., Ladenberger, A., Andersson, M., 2013. Rare earth element distribution and mineralization in Sweden: an application of principal component analysis to FOREGS soil geochemistry. *J. Geochem. Explor.* 133, 160–175. <https://doi.org/10.1016/j.gexplo.2012.10.015>.
- Scheibner, E., 1985. Suspect Terranes in the Tasman Fold Belt System, Eastern Australia. *Tectonostratigraphic Terranes Circum-Pacific Reg.* 1. pp. 493–514.
- Shokouh Saljoughi, B., Hezarkhani, A., Farahbakhsh, E., 2018. A comparison between knowledge-driven fuzzy and data-driven artificial neural network approaches for prospecting porphyry Cu mineralization; a case study of Shahr-e-Babak area, Kerman Province, SE Iran. *J. Min. Environ.* 9, 917–940. <https://doi.org/10.22044/jme.2018.6752.1495>.
- Sidorchuk, A., Märker, M., Moretti, S., Rodolfi, G., 2003. Gully erosion modelling and landscape response in the Mbuluzi River catchment of Swaziland. *Catena* 50, 507–525. [https://doi.org/10.1016/S0341-8162\(02\)00123-6](https://doi.org/10.1016/S0341-8162(02)00123-6).
- Sillitoe, R.H., 2010. Porphyry copper systems. *Econ. Geol.* 105, 3–41. <https://doi.org/10.2113/gsecongeo.105.1.3>.
- Spadoni, M., 2006. Geochemical mapping using a geomorphologic approach based on catchments. *J. Geochem. Explor.* 90, 183–196. <https://doi.org/10.1016/j.gexplo.2005.12.001>.
- Spadoni, M., Cavarretta, G., Patera, A., 2004. Cartographic techniques for mapping the geochemical data of stream sediments: the Sample Catchment Basin approach. *Environ. Geol.* 45, 593–599. <https://doi.org/10.1007/s00254-003-0926-7>.
- Templ, M., Filzmoser, P., Reimann, C., 2008. Cluster analysis applied to regional geochemical data: problems and possibilities. *Appl. Geochem.* 23, 2198–2213. <https://doi.org/10.1016/j.apgeochem.2008.03.004>.
- Tripathi, V.S., 1979. Factor analysis in geochemical exploration. *J. Geochem. Explor.* 11, 263–275. [https://doi.org/10.1016/0375-6742\(79\)90004-9](https://doi.org/10.1016/0375-6742(79)90004-9).
- Van Helvoort, P.-J., Filzmoser, P., Van Gaans, P.F.M., 2005. Sequential factor analysis as a new approach to multivariate analysis of heterogeneous geochemical datasets: an application to a bulk chemical characterization of fluvial deposits (Rhine-Meuse Delta, the Netherlands). *Appl. Geochem.* 20, 2233–2251. <https://doi.org/10.1016/j.apgeochem.2005.08.009>.
- Wang, C., Carranza, E.J.M., Zhang, S., Zhang, J., Liu, X., Zhang, D., Sun, X., Duan, C., 2013. Characterization of primary geochemical haloes for gold exploration at the Huanxiangwa gold deposit, China. *J. Geochem. Explor.* 124, 40–58. <https://doi.org/10.1016/j.gexplo.2012.07.011>.
- Wang, H., Zuo, R., 2015. A comparative study of trend surface analysis and spectrum-area multifractal model to identify geochemical anomalies. *J. Geochem. Explor.* 155, 84–90. <https://doi.org/10.1016/j.gexplo.2015.04.013>.
- Wang, W., Zhao, J., Cheng, Q., 2014. Mapping of Fe mineralization-associated geochemical signatures using logratio transformed stream sediment geochemical data in Eastern Tianshan, China. *J. Geochemical Explor.* 141, 6–14. <https://doi.org/10.1016/j.gexplo.2013.11.008>.
- Wang, W., Zhao, J., Cheng, Q., Liu, J., 2012. Tectonic-geochemical exploration modeling for characterizing geo-anomalies in southeastern Yunnan district, China. *J. Geochem. Explor.* 122, 71–80. <https://doi.org/10.1016/j.gexplo.2012.06.017>.
- Xiao, F., Chen, J., Agterberg, F., Wang, C., 2014. Element behavior analysis and its implications for geochemical anomaly identification: a case study for porphyry Cu-Mo deposits in Eastern Tianshan, China. *J. Geochem. Explor.* 145, 1–11. <https://doi.org/10.1016/j.gexplo.2014.04.008>.
- Xiao, F., Chen, J., Zhang, Z., Wang, C., Wu, G., Agterberg, F.P., 2012. Singularity mapping and spatially weighted principal component analysis to identify geochemical anomalies associated with Ag and Pb-Zn polymetallic mineralization in Northwest Zhejiang, China. *J. Geochem. Explor.* 122, 90–100. <https://doi.org/10.1016/j.gexplo.2012.04.010>.
- Xie, S., Cheng, Q., Xing, X., Bao, Z., Chen, Z., 2010. Geochemical multifractal distribution patterns in sediments from ordered streams. *Geoderma* 160, 36–46. <https://doi.org/10.1016/j.geoderma.2010.01.009>.
- Yilmaz, H., 2003. Geochemical exploration for gold in western Turkey: success and failure. *J. Geochem. Explor.* 80, 117–135. [https://doi.org/10.1016/S0375-6742\(03\)00187-0](https://doi.org/10.1016/S0375-6742(03)00187-0).
- Yousefi, M., Carranza, E.J.M., 2016. Data-driven index overlay and boolean logic mineral prospectivity modeling in greenfields exploration. *Nat. Resour. Res.* 25, 3–18. <https://doi.org/10.1007/s11053-014-9261-9>.
- Yousefi, M., Carranza, E.J.M., 2015a. Prediction-area (P-A) plot and C-A fractal analysis to classify and evaluate evidential maps for mineral prospectivity modeling. *Comput. Geosci.* 79, 69–81. <https://doi.org/10.1016/j.cageo.2015.03.007>.
- Yousefi, M., Carranza, E.J.M., 2015b. Fuzzification of continuous-value spatial evidence for mineral prospectivity mapping. *Comput. Geosci.* 74, 97–109. <https://doi.org/10.1016/j.cageo.2014.10.014>.
- Yousefi, M., Carranza, E.J.M., Kamkar-Rouhani, A., 2013. Weighted drainage catchment basin mapping of geochemical anomalies using stream sediment data for mineral potential modeling. *J. Geochem. Explor.* 128, 88–96. <https://doi.org/10.1016/j.gexplo.2013.01.013>.
- Yousefi, M., Kamkar-Rouhani, A., Carranza, E.J.M., 2014. Application of staged factor analysis and logistic function to create a fuzzy stream sediment geochemical evidence layer for mineral prospectivity mapping. *Geochemistry Explor. Environ. Anal.* 14, 45–58. <https://doi.org/10.1144/geochem2012-144>.
- Yousefi, M., Kamkar-Rouhani, A., Carranza, E.J.M., 2012. Geochemical mineralization probability index (GMPI): a new approach to generate enhanced stream sediment geochemical evidential map for increasing probability of success in mineral potential mapping. *J. Geochem. Explor.* 115, 24–35. <https://doi.org/10.1016/j.gexplo.2012.02.002>.
- Yousefi, M., Nykänen, V., 2016. Data-driven logistic-based weighting of geochemical and geological evidence layers in mineral prospectivity mapping. *J. Geochem. Explor.* 164, 94–106. <https://doi.org/10.1016/j.gexplo.2015.10.008>.
- Zhang, N., Zhou, K., 2017. Identification of hydrothermal alteration zones of the Baogutu porphyry copper deposits in northwest China using ASTER data. *J. Appl. Remote. Sens.* 11, 1–19. <https://doi.org/10.1117/1.JRS.11.015016>.
- Zhao, J., Chen, S., Zuo, R., 2016. Identifying geochemical anomalies associated with Au-Cu mineralization using multifractal and artificial neural network models in the Ningqiang district, Shaanxi, China. *J. Geochem. Explor.* 164, 54–64. <https://doi.org/10.1016/j.gexplo.2015.06.018>.
- Zheng, Y., Sun, X., Gao, S., Wang, C., Zhao, Z., Wu, S., Li, J., Wu, X., 2014. Analysis of stream sediment data for exploring the Zhunuo porphyry Cu deposit, southern Tibet. *J. Geochem. Explor.* 143, 19–30. <https://doi.org/10.1016/j.gexplo.2014.02.012>.
- Ziaei, M., Carranza, E.J.M., Ziae, M., 2011. Application of geochemical zonality coefficients in mineral prospectivity mapping. *Comput. Geosci.* 37, 1935–1945. <https://doi.org/10.1016/j.cageo.2011.05.009>.
- Zuo, R., 2011. Identifying geochemical anomalies associated with Cu and Pb-Zn skarn mineralization using principal component analysis and spectrum-area fractal modeling in the Gangdese Belt, Tibet (China). *J. Geochem. Explor.* 111, 13–22. <https://doi.org/10.1016/j.gexplo.2011.06.012>.
- Zuo, R., Cheng, Q., Agterberg, F.P., Xia, Q., 2009. Application of singularity mapping technique to identify local anomalies using stream sediment geochemical data, a case study from Gangdese, Tibet, Western China. *J. Geochem. Explor.* 101, 225–235. <https://doi.org/10.1016/j.gexplo.2008.08.003>.